Geoderma 464 (2025) 117630

Contents lists available at ScienceDirect

Geoderma

journal homepage: www.elsevier.com/locate/geoderma

Detection of short-term changes in soil clay content at field scale with Sentinel-2 enables mapping of the reservoir sediment reuse in cropland

J. Gaab [a,*], L. Ruiz [b,c], M. Sekhar [c,d], S. Dharumarajan [e], J. Masika Tutondele [a,f], M. Ebengo Okoto [a,g], C. Gomez [a]

[a] LISAH, Univ Montpellier, AgroParisTech, INRAE, Institut Agro, IRD, Montpellier, France
[b] G-eau, Univ Montpellier, INRAE, AgroParisTech, IRD, Institut Agro, Cirad, Montpellier, France
[c] Indo-French Cell for Water Sciences, Indian Institute of Science, ICWaR, Bangalore, India
[d] Indian Institute of Science, Civil Engineering Department, Bangalore, India
[e] ICAR-National Bureau of Soil Survey and Land Use Planning, Hebbal, Bangalore, India
[f] Univ. Kongo (RD Congo), Faculté des Sciences Agronomiques et Environnement, BP 202 Mbanza-Ngungu (RDC), Congo
[g] INRAE, Info&Sols, 45075 Orléans, France

ARTICLE INFO

Handling Editor: Dr Budiman Minasny

Keywords:
Soil mapping
India
Amendment
MLR method

ABSTRACT

Among the wide variety of existing agricultural practices, some amendments can lead to changes in soil properties, including those perceived as permanent, such as clay content. These modifications pose new challenges for mapping and monitoring soil characteristics. In South India, one such practice is the application of sediment from reservoirs onto agricultural fields. Our study investigates the ability of Sentinel-2 imagery to detect changes in topsoil clay content induced by this practice. We used data from a cultivated watershed in South India, including 164 topsoil samples, and a set of control fields (19 without and 43 with sediment application). Two Sentinel-2 images acquired in February and April 2017 (before and after sediment spreading) were used to estimate soil clay content via Multiple Linear Regression (MLR) models. Comparing the clay content maps from both dates revealed significant increases in areas where sediment was applied. Validation with control fields demonstrated that Sentinel-2 images successfully captured clay content changes attributable to sediment application. When extended to the entire cultivated area, our approach identified 242 fields exhibiting a significant clay increase in 2017. These results highlight the potential of multi-temporal Sentinel-2 data to monitor short-term changes in soil properties driven by agricultural practices. Future work could leverage the full Sentinel-2 archive (from 2017 onwards) to quantify long-term dynamics of sediment application across broader regions. More generally, this approach contributes to the development of Earth observation-based frameworks for tracking soil property changes associated with evolving agricultural systems at multiple spatial and temporal scales.

1. Introduction

Agricultural systems rely on a wide range of crop management practices, including, for example, soil tillage, fertilization and irrigation, which can impact crop productivity, soil sustainability, and resource management (e.g. Stamatiadis et al., 1997, Zhanguo et al., 2018). Documenting these practices in the long term at the scale of small regions or watersheds requires extensive monitoring over time and space. This type of extensive monitoring can be challenging, particularly when a significant proportion of farmers are smallholders. Field surveys are commonly used to collect such information, but their implementation is time-consuming, costly, and often limited in spatial and temporal coverage (Schapper, 1957). Remote sensing has emerged as a promising tool to complement field surveys for detecting and monitoring agricultural practices at various scales (Bégué et al., 2018). Previous studies have demonstrated its potential to identify specific practices, such as tillage (e.g., Deshpande et al., 2024), crop residue management (e.g., Daughtry et al., 2004), or irrigation (e.g., Sharma et al., 2018, Zhang et al., 2022). Sensors like LANDSAT and Sentinel-2, thanks to their high revisit frequency, may offer the possibility of monitoring agricultural practices over the course of a cropping season using time series data (Gao et al., 2020; Sharma et al., 2018).

Soil amendments (manure, biochar, sediments, etc.) have a central place in farming systems but, to our knowledge, they are rarely studied

* Corresponding author.
E-mail address: juliette.gaab@supagro.fr (J. Gaab).

https://doi.org/10.1016/j.geoderma.2025.117630
Received 17 July 2025; Received in revised form 21 November 2025; Accepted 23 November 2025
Available online 28 November 2025

with remote sensing. Dodin et al. (2021) studied the detection of green waste compost and manure amendments with spectral indices on Sentinel-2 images, and Gomez et al. (2021) detected sediment applications using soil colour changes on Sentinel-2 images. This scarcity of remote sensing studies may be due to the fact that amendments are much less frequent and widespread than other practices, such as tillage or irrigation, and therefore might only concern a small proportion of agricultural areas for a given date. However, amendments are likely to have an impact on soil properties.

Sediment application on agricultural fields is a common practice in India, where farmers spread sediment collected from reservoirs onto their fields (Gunnell and Krishnamurthy, 2003, Reddy et al., 2018). This technique is primarily used to improve soil fertility and restore degraded lands (Gunnell and Krishnamurthy, 2003, Srinivasarao et al., 2014), but also allows preservation of the capacity of reservoirs to store water. Given the significant agroecological potential of this practice in terms of circularity and sustainability of cropping systems (Gomez et al., 2025), it is important to monitor this agricultural practice and assess its impact on soils.

A first attempt to use remote sensing for mapping reservoir sediment application was carried out in South India (Gomez et al., 2021). It was based on the observation that the practice often leads to a visible shift in top soil colour, from red (typical of Ferralsols and Chromic Luvisols) to darker brown shades because of the dark colour that often characterises the sediments. Using two Sentinel-2 multispectral images, at the beginning and at the end of the dry season, these authors successfully identified fields that had received sediment, with good accuracy. Although interesting and innovative, this approach has several limitations. First, it lacks genericity, as it can apply only to cases where sediment and soils have clearly distinct colours. Second, the information provided by this approach is limited to identifying the occurrence of the application, but not to quantify the magnitude of its impact on soil properties.

Actually, given the often very large doses of sediment input (Gomez et al., 2025; Reddy et al., 2018), this practice is likely to modify profoundly the soil properties, in particular their texture, as the proportion of clay is often much greater in the sediment than in the soils where they are applied (Canet et al., 2003, Deshmukh et al., 2019, Gomez et al., 2025). While soil texture is usually considered a 'stable' property—changing only over pedological timescales (Wilding et al., 1994)—in the case of sediment application, it becomes a dynamic property, meaning it may vary over human timescales (from hours to decades) as a result of land use and management (Tugel et al., 2005).

It has been largely demonstrated that clay content can be estimated by Laboratory Visible-Near Infrared (Vis-NIR, 400–2500 nm) spectroscopy (e.g., Chabrillat et al., 2002, Kariuki et al., 2004). Beyond Lab spectroscopy, Vis-NIR satellite optical remote sensing has also been successfully used to estimate and predict spatially surface clay content at large extents, with satisfactory accuracy (e.g., Castaldi et al., 2023; Gasmi et al., 2021). These remote sensing approaches are valuable tools to map the spatial organization of soil properties such as clay content across landscapes. Studies have shown that pedological patterns and prediction ranges remain consistent across different remote sensed observation datasets (Gasmi et al., 2022; Gomez et al., 2018; Žížala et al., 2019). However, the accuracy of soil properties mapping from remote sensing data can be influenced by several environmental factors. Since the presence of vegetation on the ground can significantly affect the model accuracy and therefore soil properties predictions, as shown by Bartholomeus et al. (2011) and Ouerghemmi et al. (2011; 2016), prediction models are strictly calibrated and applied to bare soil pixels. Over these bare soil pixels, the regression performances remain acceptable and consistent regardless of other environmental factors (moisture, roughness or atmospheric conditions), provided that images are acquired under dry soil conditions and on cloud-free days (Gomez et al., 2019, 2022; Vaudour et al., 2019b). Hence, the question remains as to whether remote sensing can be sufficiently sensitive to observe changes in soil properties due to land use and management at the watershed scale.

Therefore, in this paper, we tested the hypothesis that an anthropogenic intervention, such as sediment application, which causes a change in soil clay content, can be detected by comparing optical remote sensing images taken before and after the intervention. This requires that this change be significantly greater than the variations in estimated clay content between these two dates due to environmental or instrumental disturbances.

We focused on a study area in peninsular India, using two Sentinel-2 images, taken at the beginning and the end of the dry season, during a year (2017) when reservoirs were dry, allowing farmers to apply sediment to agricultural fields. The study has three key objectives: i) determine the threshold of change in clay content above which the practice can be identified, ii) identify agricultural fields where sediment was applied in the watershed and compare the results with the approach based on soil colour change detection and iii) quantify a surface area impacted by the practice during the dry season, more specifically between 2017-02-03 and 2017-04-24.

2. Materials and methods

2.1. Study area

This study focuses on the Berambadi watershed, which is located on the Deccan Plateau in South India in the Chamarajanagar district, in the state of Karnataka (Fig. 1a). The Minimum Bounding Box (smallest rectangle aligned with the coordinate axes which enclose all observations) of the watershed is defined by the following coordinates: Northern limit: 11° 48′ 56.86 N, Southern limit: 11° 43′ 30.10 N, Eastern limit: 76° 39′ 39.38 E and Western limit: 76° 30′ 52.86 E. This watershed belongs to the Kabini Critical Zone Observatory (Sekhar et al., 2016; Tomer et al., 2015; AMBHAS Team, 2015), which is part of the OZCAR network (Gaillardet et al., 2018). The Berambadi watershed covers about 84 km^2 and is divided into 2 zones: the western part (around 40 % of the watershed) covered by a dry deciduous forest and the eastern part dominated by arable lands. The monsoon dynamics determine three cropping seasons: the dry season (also called "summer season", from January to May), the kharif season (southwest monsoon season, from June to September) and the rabi season (north-east monsoon season, from October to December). The climate is tropical subhumid with an average precipitation (P) of 800 $mm.year^{-1}$ and a potential evapotranspiration (PET) of 1100 $mm.year^{-1}$ (aridity index P/PET of 0.7) (Sharma et al., 2018). Meteorological variables are recorded hourly since 2004 over this watershed, with an automatic weather station (Sekhar et al., 2016).

The watershed has a wide variety of cropping systems, with both rainfed and irrigated fields. Groundwater irrigation appeared in the 1970s and expanded significantly in the area in the 1990s with the multiplication of borewells and pumps, which has not stopped since (Fischer et al., 2022). Presently, around 60 % of farmers in the watershed have access to irrigation on at least one of their fields (Robert et al., 2017). The presence of irrigation had an impact on cropping systems, as it has enabled irrigating farmers to cultivate during the dry season. Previous typology studies defined 3 different types of farms in the study zone: large diversified and productive farms; small and marginal rainfed farms, and small irrigated marketing farms (Robert et al. 2017). Several strategies exist among farmers with irrigation: some farmers grow primarily short-cycle crops (around 3 months) such as vegetables, onion, garlic or cabbage for 2 or 3 seasons depending on water availability, while some farmers combine long-cycle crops (9 to 12 months) with short-cycle crops within their farms (Baccar et al., 2023).

In the watershed, the soil texture of uplands and hillslopes is predominantly coarse (Sandy Loam) because of erosion processes. In contrast, the soil texture of valley bottoms is generally more clayey because of deposition processes (Barbiero et al., 2010, Gomez et al.,

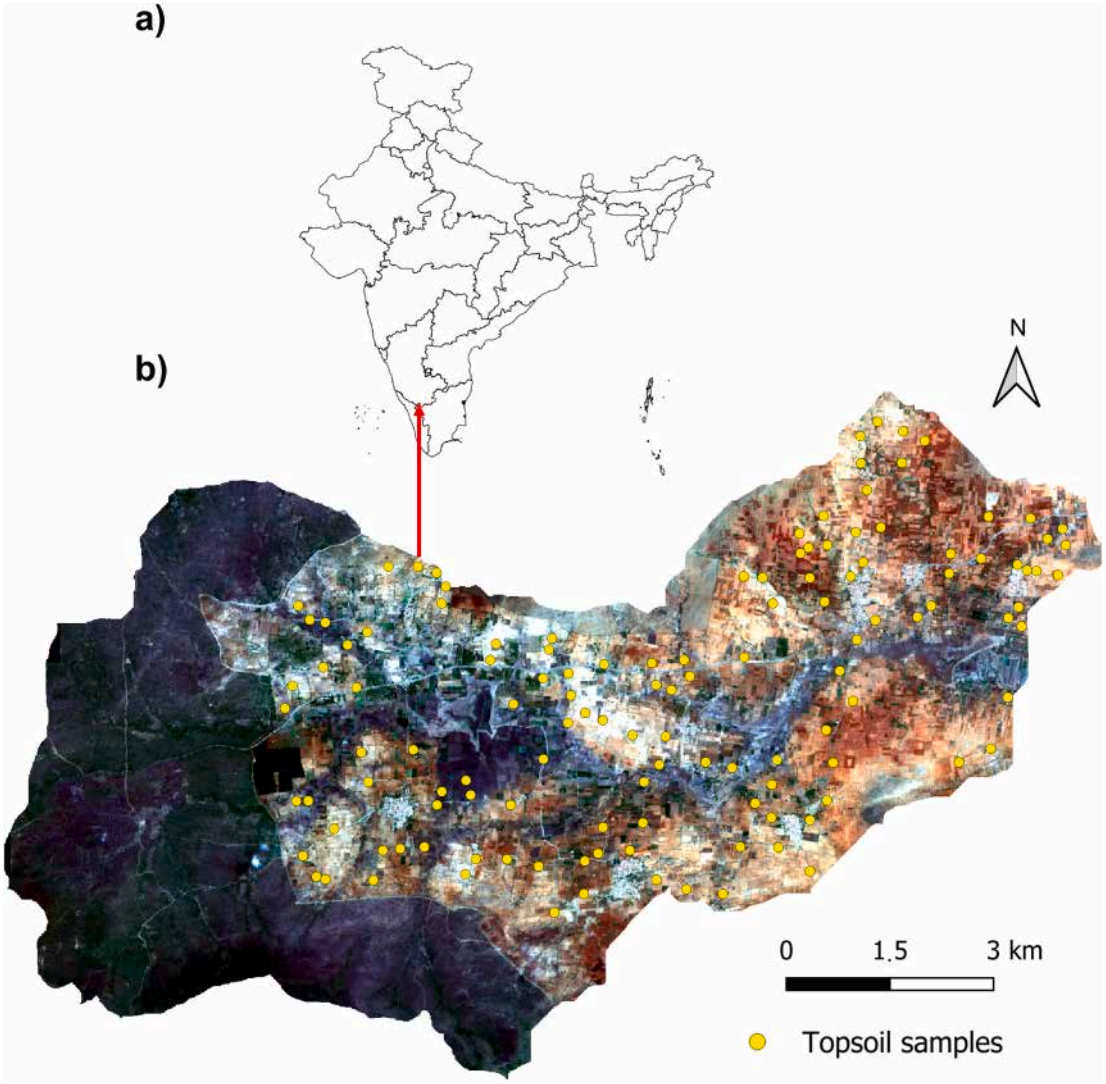

Fig. 1. a) location of the Berambadi watershed in India (Karnataka State) and b) 125 topsoil samples collected in field located on the Sentinel-2 image (in false colour) acquired on 3rd of February 2017.

2019).

The Berambadi watershed includes 40 reservoirs, of which at least 14 are known to be used for sediment application (Gomez et al., 2025).

2.2. Sediment reuse on agricultural fields

In the Berambadi watershed, as in other regions of India, reuse of sediment from water reservoirs over croplands is a centuries-old practice (DHAN foundation 2012). In the past, farmers would dig into the bottom of the reservoirs when they were empty to collect sediment and transport it using bullocks (DHAN foundation 2012, Hemingway et al., 2025). The recent development of motorisation has facilitated a broader spatial expansion of this practice (DHAN foundation 2012). Presently, sediments are extracted from the reservoirs with excavators, transported with tractors and deposited in piles on agricultural fields, typically for a few days, rarely for a few weeks, according to the availability of the leveller, before being incorporated into the soil with ploughing work, at a depth of around 30 cm.

Previous analyses of sediments originating from reservoirs over Berambadi exhibit contrasting granulometry from one reservoir to another (Gomez et al., 2025), as while their silt contents were around 20 %, the clay and sand contents were variable. In addition, physico-cheminal analyses on couples of soil and sediment collected in farmer's fields highlighted that significant differences between soil and sediment were observed for clay, sand, P, CEC, TN and C/N (Gomez et al., 2025). Finally, the reflectance spectra acquired on soils, sediments, and a mixture of soil and sediment, in the visible and near-infrared (Vis-NIR, 400–2500 nm) spectral range by laboratory spectroscopy, are very similar in shape, with the same absorption band around 2206 nm (Supplementary figure S3) which corresponds to clay minerals (Chabrillat et al, 2002).

One of the particularities of the practice of sediment reuse is its temporality, which is linked with the availability of sediments: they are only accessible during the dry season, from January to May, once the reservoirs are empty of water (Gomez et al., 2025). The sediment application season ends after the first convective rains occurring during the last part of the dry season (April or May).

2.3. Sentinel-2 images

Launched in 2015 and then in 2017, both Sentinel-2A and Sentinel-2B satellites provide multispectral images every five days at the equator. The reflectance is acquired in 13 spectral bands within the Visible Near Infrared (Vis-NIR, 0.4–2.5 μm) spectral domain, with a spatial resolution from 10 to 60 m. Two Sentinel-2 images covering the Berambadi watershed, which have previously been described and utilised in Gomez

et al. (2019), were chosen for this study. The acquisition dates were chosen based on two main criteria. First, it was essential to capture one image at the beginning of the dry season, before sediment applications, and another at the end of the dry season, after sediment applications. Second, the selection was guided by the absence of rainfall in the days preceding the acquisition, as precipitation increases soil moisture, which in turn affects the reflectance spectrum and the estimation of clay content.

Following these criteria, and using rainfall data from the automatic weather station, the first Sentinel-2 image was acquired on February 3, 2017, after six consecutive days without rainfall, while the second was captured on April 24, 2017, following three rain-free days. Although we will possibly miss some early or late sediment applications, we can assume that the vast majority of them are occurring between these two dates. As a consequence, we can assume that the quantification of the spatial extent of the practice will be only slightly underestimated.

Atmospheric and topographic corrections were performed with the MAJA processor (Hagolle et al., 2017; Lonjou et al., 2016) on-demand PEPS (Plateforme d'Exploitation des Produits Sentinel) processing service, which uses eight Sentinel-2 acquisitions prior to each acquisition of interest to meet the temporal assumption (https://labo.obs-mip.fr/multitemp/on-demand-sentinel2-l2a-processing-with-maja-on-peps). Ten bands remain after atmospheric correction, and the six spectral bands initially acquired with 20 m spatial resolution were resampled to 10 m. Using the function "disaggregate" from the package "raster" in R, the spatial resampling preserved the original values in the new, higher-resolution raster layer. In order to keep only bare soil pixels, the roads, urban and water areas were first masked using a land use map available for the study area (e.g., AMBHAS Team, 2015). Then, the normalized difference vegetation index (NDVI), calculated using spectral bands at 865 nm and 665 nm (Frampton et al., 2013; Rouse et al., 1973), was used to mask crops and natural vegetation, based on a threshold of 0.3 derived from the visual evaluation of an expert with significant field knowledge (Gomez et al., 2022). In addition, the Normalized Burned Ratio 2 index (NBR2), calculated using the SWIR1 band B11 (1610 nm) and the SWIR2 band B12 (2202 nm), was used to mask pixels corresponding to crop residue and moist soil (Deventer et al., 1997). While the NBR2 index was initially developed for LANDSAT data and in a temperate context, recent studies have validated its use with Sentinel-2 data both in temperate (e.g., Castaldi et al., 2023, Dvorakova et al., 2023) and tropical context (e.g., Silvero et al., 2021; Pérez et al., 2022). A threshold of 0.15 was used, based on the previous work of Gomez et al. (2022) dedicated to the same study area.

Finally, only the common bare soil pixels of both images were selected for further studies, representing 88 % of the cultivated areas, evenly distributed throughout the watershed.

2.4. Topsoil samples with clay content

In November 2019, we collected 164 topsoil samples over the Berambadi watershed on agricultural fields without sediment application between 2017 and 2019. The sampling followed the sampling design detailed in Gomez et al. (2022), ensuring it was representative of the study area and covered the full range of soil types. Among these samples, 125 topsoil samples were located over bare soil pixels on both Sentinel-2 images and were evenly distributed on the watershed (Fig. 1b). These 125 samples were kept for building regression models of clay content prediction. Each sample was composed of 5 subsamples taken at a depth of 5 cm within a 10 m × 10 m square centered according to the geographical position of the sampling field. The 5 subsamples (1500 g in total) were then mixed and 20 g were extracted to be air-dried and sieved at 2 mm. We used the pipette method, as described by Piper (1966), to estimate the clay content of the samples. The clay content of these 125 samples ranged from 5.8 to 59.2 % with a mean of 22.5 %, a standard deviation of 11.5 % and a skewness of 0.6 %.

In a previous study dedicated to the same area, Gomez et al. (2025) showed that the soil clay content before sediment application ranged from 10.9 to 51.1 % with a mean of 30.0 %, while the clay content of soil recently mixed with sediment ranged from 33.9 to 50.5 % of clay content with a mean of 41.6 % (See Supplementary Table 1 in Gomez et al. 2025). So, although the model was trained only on samples from fields without sediment application, our 125 soil samples cover a wide range of clay content, encompassing both soils with no sediment applications and soils recently mixed with sediment.

As soil clay content is a property that remains stable over time in the absence of sediment application, Sentinel-2 images acquired in 2017 and topsoil samples collected in 2019 can be used together to build clay content prediction models, as reported in many previous studies (e.g., Castaldi, 2021; Castaldi et al., 2023; Vaudour et al., 2021; Žížala et al., 2019).

2.5. Control fields

Using three high-resolution images available on GoogleEarth, acquired on 2017–02-23, 2017–02-24 and 2017–02-27 (Google Earth Pro, 2025), we visually identified 57 agricultural fields with piles of sediment and delineated their boundaries (Fig. 2a). Indeed, the ground surface of a pile of sediment is estimated to be around 5 m^2 and are often black and contrasting with the red colour of the soil (Gomez et al. 2025). Both the distinction in colour and their volume makes the piles easily identifiable on Google Earth (see Fig. 2b and Supplementary Fig. S5). There is a possibility that some of these 57 applications occurred before the 2017-02-03 (date of our first Sentinel-2 image). However, this seems unlikely, as field observations indicate that sediment piles are typically left in the field for only a few days before being incorporated. Among these 57 agricultural fields, 14 contain less than 30 % pixels identified as bare soil, and were therefore excluded from the analysis due to insufficient bare soil coverage. The remaining 43 fields, with at least 30 % bare soil pixels, were used as control fields with sediment application. Their mean surface area is 0.32 ± 0.17 ha. We also identified 19 agricultural fields with at least 30 % bare soil as control fields without sediment application in 2017 based on farmer interviews. Their mean surface area is 0.38 ± 0.16 ha. To account for potential misalignment between field boundaries and the clay raster maps, an inner buffer of 5 m was applied to all control fields (43 with sediment application and 19 without), ensuring a more accurate analysis by reducing edge-related discrepancies. On average, the implementation of this buffer decreases the number of bare soil pixels taken into account in these control fields by 37 %.

Following the spectral response observed in Lab (Supplementary Fig. S3), we also observed that Sentinel-2 spectral responses of the control fields without sediment and of the control fields having received sediment, appear relatively similar, with lower reflectance for sediment and soil mixture than soil (Supplementary Fig. S4B). Finally, the S2 spectra of both February (Supplementary Fig. S4C) and April (Supplementary Fig. S4D) from the two groups (control fields which never received sediment and control fields which received sediment application before April) fall within the range of the dataset used to train the regression models. It indicates that they share similar overall characteristics with the training data and that the PCA model provides an appropriate representation for their projection. Their position suggests that no major structural differences or atypical patterns distinguish them from the original dataset on the first two principal components.

2.6. Agricultural field delineation

For identifying the fields over which sediment was applied in 2017, we used an agricultural field delineation of the Berambadi watershed in 2017, which was first produced for the study zone in 2014 and then updated using Google Maps tiles dating from January 2017 (Sharma et al., 2018). This delineation contains 16,612 polygons, which belong to the category "agricultural land". As with the control fields, to account

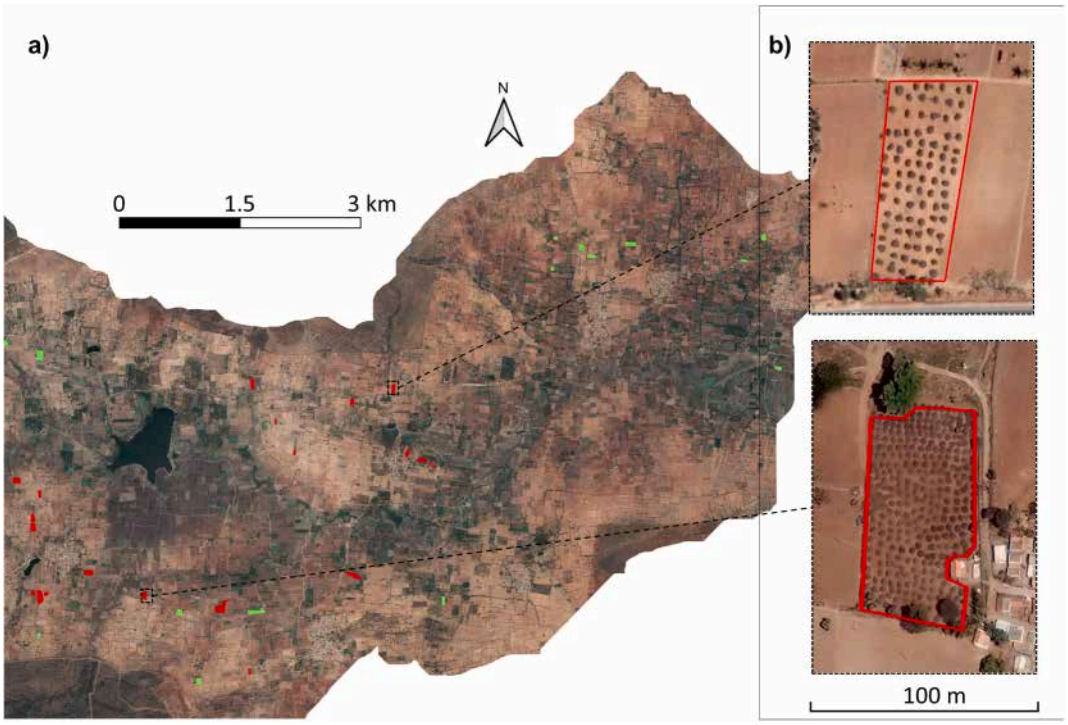

Fig. 2. a) 19 control fields without sediment in 2017 (green polygons) and 43 control fields with sediment application (red polygons), b) zoom on two control fields with piles of sediments detected on GoogleEarth on the 23/02/2017, 24/02/2017 and 27/02/2017.

for potential misalignment between agricultural field delineation and the clay raster maps, an inner buffer of 5 m was applied to all polygon boundaries, ensuring a more accurate analysis by reducing edge-related discrepancies. On average, the implementation of this buffer decreases the number of bare soil pixels taken into account in the agricultural field delineation by 32 %. Furthermore, only agricultural fields with at least 5 bare soil pixels and a minimum of 30 % bare soil coverage were retained for the analysis. This selection resulted in a total of 10,925 fields, with an average area of 0.31 $\pm$ 0.21 ha. The control fields presented in section 2.5 have a mean surface area that is statistically similar to the entire agricultural field delineation. Thus, there is no size bias in the fields used as control and they are representative of the entire fields in the watershed.

2.7. Map of soil colour change to detect sediment application

Sediment applications have already been detected with a map of soil colour change produced using the same Sentinel-2 images, based on the hypothesis that a change of soil colour from "Red" (characteristic of Ferralsol) in February 2017 to "Black" (characteristic of most of the sediment) in April 2017 could be attributed to sediment application (Gomez et al., 2021).

The change of soil colour between both dates was estimated based on a bootstrap procedure providing 50 classifications for each Sentinel-2 image. The mean of frequency of changes over the 50 iterations was calculated at the field scale and high and positive values (from 40 to 50 iterations) corresponded to a significant change of soil colour from "Red" to "Black".

The map of soil colour changes in Gomez et al. (2021) was produced after masking only green vegetation, but not dry vegetation as in this study. In order to compare similar surfaces of bare soil pixels, we intersected the map of soil colour changes with the filtered Sentinel-2 images used in this study.

2.8. Regression models

The Multiple Linear Regression (MLR) method was chosen to construct clay content prediction models (Montgomery et al., 2012) following several previous studies (e.g., Gomez et al., 2022; Mirzaee et al., 2016; Wang et al., 2022b) which take benefit from the straightforward intuitive interpretation, efficiency and simplicity of this MLR method. Sentinel-2 reflectance data were used as predictors (10 spectral bands) in the MLR models and the clay content data from topsoil samples selected over corresponding bare soil pixels were used as response variables (1 soil property). One MLR model was built from each Sentinel-2 image and each MLR model was then applied to bare soils pixels of the corresponding Sentinel-2 image to obtain a clay map at each date (Fig. 3a).

The initial dataset of 125 couples of clay content and Sentinel-2 reflectance data over bare soil pixels was divided into a calibration dataset (3/4 of the initial dataset) and a validation dataset (1/4 of the initial dataset). The clay contents were sorted in ascending order, and the sample with the lowest clay content was put into the validation dataset. This process was repeated iteratively: every fourth sample was placed into the validation set, and the others into the calibration set. This approach ensured that both the calibration and validation sets exhibited comparable distributions of clay content. Spectral outliers were investigated in the calibration datasets for each date (Wold et al., 2001). The spectral outliers were identified by applying the Mahalanobis distance (Mark and Tunnell, 1985) to data condensed by principal component analysis (PCA). A Mahalanobis distance of 3.5 was selected as the threshold for the identification of spectral outliers. If a sample corresponding to a spectral outlier was identified for one date, it was removed from both datasets in order to build the models on the same datasets and obtain comparable results.

Performances of both regression models were assessed on the calibration dataset using both the coefficient of determination (R^2_{cal}) and the Root Mean Square Error ($RMSE_{cal}$). They were also assessed on the validation dataset using the coefficient of determination (R^2_{val}), the Root Mean Square Error of prediction (RMSEP), the ratio of the performance

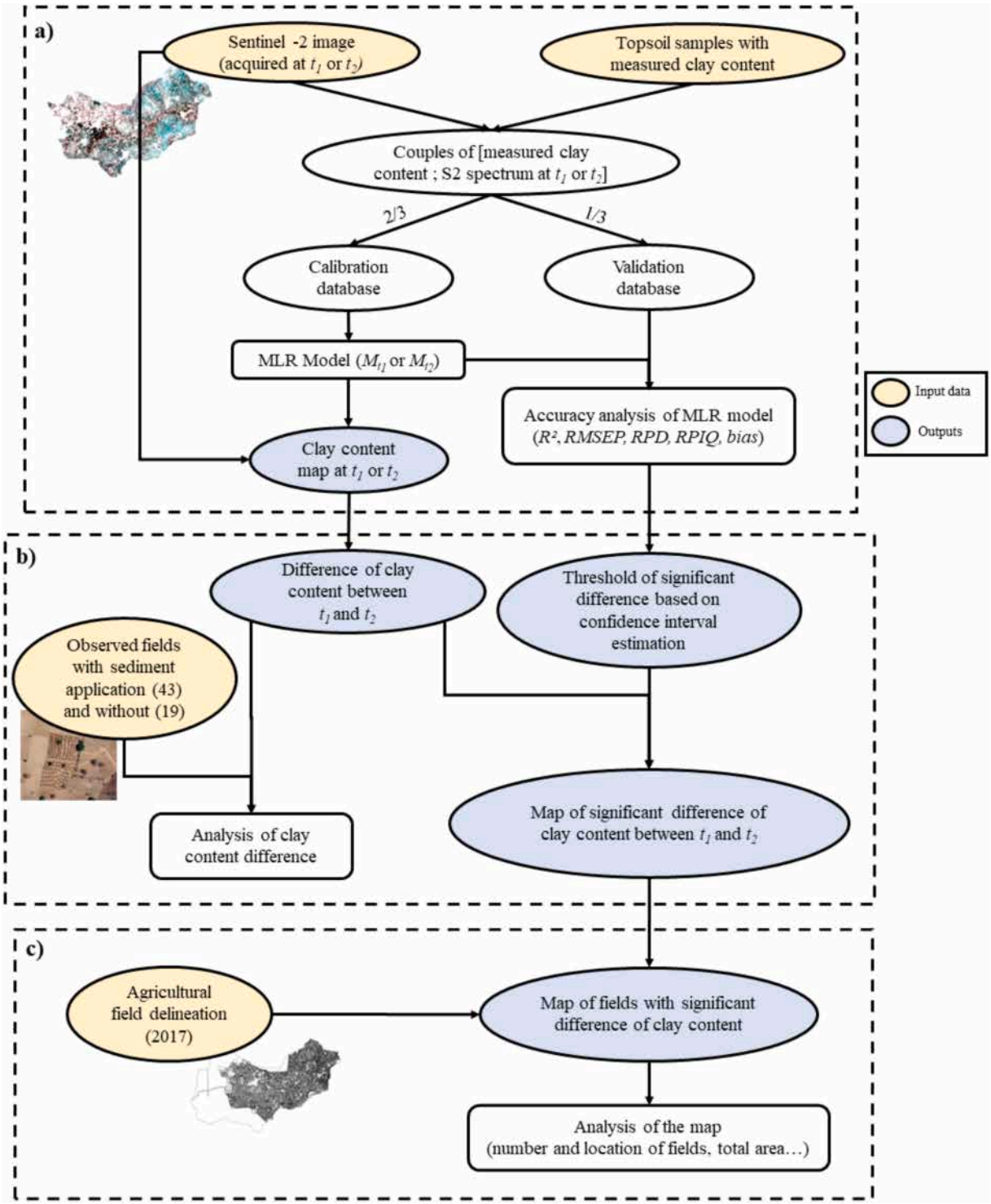

Fig. 3. Workflow of sediment applications mapping based on a couple of Sentinel-2 images for the dates: t_1 = 03/02/2017 and t_2 = 24/04/2017.

to the deviation (RPD) and the Ratio of Performance to Interquartile distance (RPIQ) (Bellon-Maurel et al., 2010) (Fig. 3a). According to Chang et al. (2001) and Viscarra Rossel et al., (2006), RPD values between 1.4 and 1.8 indicate models with moderate predictive performance, values between 1.0 and 1.4 indicate poor predictive performance, and values below 1.0 correspond to very poor models. Based on this ranking system, RPIQ values below 1.89 indicate unsuccessful estimations, whereas values up to 2.7 correspond to good estimations.

Both clay content maps obtained by applying the MLR model M_{ti} to the corresponding image acquired at t_i (Fig. 3a), were analysed and compared. The bias between the clay contents predicted in February and April was calculated as follows:

$$Bias = \sum_{i=1}^{n} \frac{\hat{y}_{i,t_2} - \hat{y}_{i,t_1}}{n} \quad (1)$$

where n is the number of bare soil pixels, $\hat{y}_{i,t_2}$ the predicted clay value obtained on 2017–04-24 (t_2) over the pixel i and $\hat{y}_{i,t_1}$ the predicted value of clay on 2017–02-03 (t_1) over the same pixel i.

Finally, the difference in predicted clay content ($Diff_j$) between both images was calculated for each pixel (Fig. 3b) using the following approach:

$$Diff_j = \hat{y}_{j.t_2} - \hat{y}_{j.t_1} \quad (2)$$

where $\hat{y}_{j.t_2}$ is the predicted clay content value of the pixel j on the 24th of April 2017 and $\hat{y}_{j.t_2}$ the predicted clay content value of the pixel j on 2017–02-03.

Regression models and analysis were performed using R software (R Development Core Team, 2012), and both the ade4 (Dray and Dufour, 2007) and pls packages (Mevik and Wehrens, 2007) were used.

2.9. Confidence interval estimation

A confidence interval, which reports the range of values within the true value is expected (Heuvelink, 2014), was calculated (Fig. 3b). The lower and upper confidence interval limits are designated as CI_{inf} and CI_{sup}, respectively. For a pixel j, the difference $Diff_j$ in predicted clay contents between t_1 and t_2 is considered:

- non-significant and is attributed to MLR models errors if $CI_{inf} < Diff_j < CI_{sup}$,
- significant if $Diff_j$ exceeds the confidence interval with $Diff_j > CI_{sup}$ which truly reflect sediment application and not changes in surface conditions that may also affect reflectance,
- significant if $Diff_j < CI_{inf}$ but for which MLR models errors may not explain such difference between both dates.

The confidence interval was calculated based on the residuals X_1 of the model M_{t1}, i.e the difference between the measured and the predicted values at t_1 for the validation dataset, and the residuals X_2 of the model M_{t2} i.e the difference between the measured and the predicted values at t_2 for the validation dataset, as proposed by Styc (2020):

$$CI_{inf} = \overline{y}_{X_2-X_1} - 1,162\sigma_{X_2-X_1} \quad (3)$$

$$CI_{sup} = \overline{y}_{X_2-X_1} + 1,162\sigma_{X_2-X_1} \quad (4)$$

where CI_{inf} is the lower interval limit of the difference, CI_{sup} is the upper interval limit of the difference, $\overline{y}_{X_2-X_1}$ is the mean of the distribution of $X_2 - X_1$, $\sigma_{X_2-X_1}$ is the standard deviation of $X_2 - X_1$ and 1.162 is the Student's coefficient for a 90 % confidence interval estimation corresponding to our number of topsoil samples representing the measured data.

Finally, a map highlighting significant differences in clay content between t_1 and t_2 was created with only the pixels where the clay content difference $Diff_j$ was either below CI_{inf} or above CI_{sup} (Fig. 3c).

2.10. Criteria for detection of fields with a significant difference in clay content

In our study, a field f shows a significant difference of clay content between the two dates if it meets the following criteria: both the mean and median differences in clay content of the field are above CI_{sup}. or both under CI_{inf}. Using the median clay difference helps to exclude fields where a few outlier pixels strongly influence the mean difference. Conversely, the mean clay difference helps to capture fields where a subset of pixels shows distinctly different clay values from the rest, i.e. with patterns that would not be detected by the median alone.

If both mean and median differences are positive and above $CI_{sup.}$ we considered that the field f presents a significant increase in clay content associated with a sediment application. If these differences are negative and under CI_{inf}, we considered that the field f presents a significant decrease in clay content. An analysis of control fields (with and without sediment application) was conducted to validate our approach (Fig. 3b). Then, these criteria were used to detect fields with sediment application between t_1 and t_2 at watershed scale, based on the agricultural field delineation of the Berambadi watershed (section 2.6) and also to detect fields with a significant decrease in clay content.

We carried out Wilcoxon Signed-Rank tests (non-parametric test) in order to compare the average clay content between different field groups (fields with a significant increase in clay content, fields with a significant decrease in clay content and fields with no significant variation).

2.11. Comparison with soil colour change map

To test the robustness of our method compared to the soil colour change map, we compared fields detected with a significant difference in clay content and fields detected with a significant change of colour based on the map of soil colour changes produced in Gomez et al. (2021). Both control fields and the agricultural fields delineation were studied with both methods. Among the 43 control fields with sediment application, only 42 could be studied with the soil colour change map, as one field has no bare soil pixel on this map due to the difference in the mask applied to the original Sentinel-2 images.

We applied similar criteria (mean and median above the significant threshold determined in Gomez et al., 2021) to the map of soil colour changes to detect fields with a significant difference. Thus, a field f was considered as having received sediment if both the mean and median changes from "Red" to "Black" exceeded 40 across the 50 iterations (significant threshold in Gomez et al., 2021). Similarly, a field f presented a significant change of colour from "Black" to "Red" when both the mean and median changes from "Black" to "Red" exceeded 40 across the 50 iterations. An analysis of the 42 control fields with sediment application and the 19 control fields without sediment on the colour change map was conducted to compare with our approach. We carried out Wilcoxon Signed-Rank Test (non-parametric test) to compare the average clay content between the fields with both significant difference with the clay content approach and the colour change approach and the fields showing a significant change only in clay content.

3. Results

3.1. Regression models performances

No spectral outlier was identified in the calibration dataset built from the image acquired on 2017-04-24 and two spectral outliers were identified in the calibration dataset built from the image acquired on 2017-02-03, reducing the calibration dataset from 96 initially to 94 data points for both models. Both MLR models were built, first trained by the calibration dataset (94 couples of spectrum acquired either on 2017-02-03 or 2017-04-24, and associated measured clay content) and validated on the validation dataset (31 couples of spectrum acquired either on 2017-02-03 or 2017-04-24, and associated measured clay content) (Fig. 3a). The Sentinel-2 spectra of these 125 bare soil pixels presented different intensity but similar shape with the typical increase of reflectance from VIS (B02) to SWIR (B12) bands, with a peak at the SWIR1 band (B11) (Supplementary Fig. S4A), as observed in Vaudour et al. (2019a).

The performances of the models were similar according to the R^2 and RMSE values, for both calibration and validation steps (Table 1, Supplementary Fig. S1 and Fig. S2). According to the criteria defined in Section 2.8, the RPIQ and RPD values are also satisfactory.

3.2. Predicted clay content maps

Each model was applied to common bare soil pixels of the corresponding Sentinel-2 image, evenly distributed throughout the watershed (Fig. 4a). This process led to two clay content maps with a clay value for every bare soil pixel on 2017-02-03 (Fig. 4a) and on 2017-04-24

Table 1
Figures of merit obtained with both MLR models built from Sentinel-2 images acquired in February and April. The statistics used are: R^2 = coefficient of determination; RMSE = root mean square error; RMSEP = Root Mean Square Error of prediction; RPIQ = ratio of performance to interquartile range and RPD = ratio of the performance to the deviation.

	Calibration		Validation			
	R^2_{cal}	$RMSE_{cal}$ (%)	R^2_{val}	RMSEP (%)	RPIQ	RPD
2017–02-03	0.76	5.71	0.71	6.15	2.55	1.79
2017–04-24	0.77	5.62	0.75	5.55	2.82	1.99

(Fig. 4b). For both maps, we observed a similar spatial pattern between both maps, with low clay contents (around 20 %) located in the uplands and hillsides, whereas higher predicted clay contents (which may exceed 50 %) were located in the valleys (Fig. 4a). These maps have a close clay content distribution (Fig. 4c) with similar skewness (0.5 in February and 0 in April), mean (24.5 % in February and 24.2 % in April), and standard deviations (10.0 % in February and 10.2 % in April). They both follow a normal distribution and there is no bias between predicted values at both dates (bias of −0.23 %), which proves that different intensities between spectra acquired at both dates (Supplementary Fig. S4A) do not affect the predictions. This distribution shows that, while there are two major soil types in the watershed, there were no bimodal patterns in clay content distribution but rather a continuum centred at 24 % of clay content.

3.3. Analysis of significant clay content differences

The CI_{inf} and CI_{sup} (Eqs. (3) and (4)) determining the threshold of predicted clay content differences that are considered significant were equal to −9.8 % and 9.8 %, respectively. So, a field *f* was considered as having received sediment if both the mean and median difference in clay content of the field were above 9.8 %. A map of the clay content variation between 2017–02-03 and 2017–04-24 at the watershed scale was produced, highlighting the pixels showing a significant variation (Supplementary Fig. S6).

3.3.1. Validation of the method with control fields

There are 18 control fields without sediment application with a clay content difference within the confidence interval [CI_{inf}; CI_{sup}] (Table 2), meaning that 95.0 % of our 19 control fields were successfully considered as not having received sediment based on these predicted clay content analyses. These 18 fields showed a mean increase of 2.7 ± 2.9 % in clay content and a mean predicted clay content in February of 29.7 ± 9.3 %. The remaining control field showed a mean and median difference in clay content slightly above CI_{sup} (10.0 and 10.2 % respectively). Therefore, the risk of getting false positive results when using this method to detect sediment application is relatively low.

Among the 43 control fields with sediment application, 38 fields (i.e. 88.4 %) were successfully considered as having received sediment based on the difference in clay contents estimated between both dates (Table 2). These 38 fields present a mean increase of 19.3 ± 6.3 % in clay content, which is more than twice the significant threshold, showing that sediment application can have a strong impact on soil texture. The mean predicted clay content in February for these 38 fields was 19.9 ± 6.8 %, i.e. slightly lower than the average clay content at watershed scale in February (24.5 %).

The 5 remaining control fields with sediment application displayed no significant difference in clay content between both dates with a mean increase of 1.9 ± 7.1 % of clay content. These fields had a greater clay content in February compared to the other control fields: 43.0 ± 5.9 %. This high clay content prior to the sediment application may explain why the addition of sediment was not sufficient to raise the clay content above the threshold, especially if we consider that the mean clay content of sediment measured in Gomez et al. (2025) is 48.1 %.

3.3.2. Analysis at watershed scale

Based on the agricultural field delineation from 2017, our method allowed to identify 242 fields having received sediment (orange polygons, Fig. 5). These fields represented a total area of 76.2 ha and were evenly distributed over the entire cultivated area of the watershed (Fig. 5). Their mean increase in clay content was 15.4 ± 6.4 %. The interquartile range indicated that 50 % of the observed increases laid between 10.9 % (Q1) to 17.9 % (Q3) (Fig. 6a). The mean predicted clay content of these fields in February was 21.0 ± 8.3 % (Fig. 6b). We detected sediment applications even for fields with an initial clay content greater than 35 % which are considered as highly clayey fields. This was not the case among the control fields with sediment application, where the 5 fields which were initially highly clayey were not detected. As sediment from different reservoirs in the area show a wide range of clay content (Gomez et al., 2025), even highly clayey fields receiving applications can be detected by our method if the sediment is particularly rich in clay.

We identified 208 fields as having a significant decrease of clay content from February to April (blue polygons, Fig. 5). These fields represented a total surface area of 56.4 ha and were mostly present on the North East of the Berambadi watershed (Fig. 5). Their mean clay content decrease was − 11.8 ± 1.6 % (Fig. 6a), and the interquartile range indicated that 50 % of the observed decreases laid between −12.6 % (Q1) and −10.3 % (Q3). Hence, compared with fields with a significant increase in clay content, the range of decrease was much narrower. Moreover, their mean predicted clay content in February was 30.1 ± 6.7 % (Fig. 6b), i.e. statistically higher than the average of fields with no significant variation (24.4 ± 9.6 %) (Wilcoxon Signed-Rank tests, p-value = 2.2e-16) and the 242 fields with a significant increase in sediment application (21.0 ± 8.3 %) (Wilcoxon Signed-Rank tests, p-value = 2.2e-16).

3.4. Comparison with sediment application detection based on soil colour changes

Based on the soil colour change map, 18 of the 19 control fields without sediment application presented no soil colour changes from February to April (Table 3). Among the 42 fields with sediment application, only 17 fields met the criteria leading to a change from “Red” to “Black”, attributed to a sediment application (Table 3). None of the remaining 25 fields met the inverse criteria leading to a change from “Black” to “Red” (Table 3), while 22 of these fields were detected as having received sediment application from the clay content variation analysis. Thus, it can be concluded that the detection of sediment application based on a variation of clay contents from February to April is a more consistent method than the one based on soil colour change.

Among the 242 fields detected with a significant increase of predicted clay content, 221 could be studied with the soil colour change map while the other 21 did not match 30 % of coverage in bare soil with the soil colour change map. Among these 221 fields, 69 were also detected with a soil colour change from “Red” to “Black” while the remaining 152 fields were not associated to a soil colour change.

The clay content predicted in February was significantly lower for the 69 fields exhibiting changes in both clay content and colour than for the 152 fields exhibiting only a change in clay content but not in colour change (Wilcoxon Signed-Rank tests, p-value = 4.913e-07) (Fig. 7b). Moreover, the clay content increase was significantly higher for the 69 fields exhibiting changes in both clay content and colour than for the 152 fields exhibiting a change in clay content but not in colour (Wilcoxon Signed-Rank tests, p-value = 4.353 e-06) (Fig. 7a). The distribution of predicted clay content in February according to their soil colour classification from Gomez et al. (2025), shows that half of the soils classified as “Red” exhibit clay content predicted in February from 13.4 % (Q1) to 21.9 % (Q3) with an average of 17.5 % (Fig. 8), while soils classified as “Black” have a higher clay content, with a mean of 31.9 %, with half of the values ranging from 26.9 % (Q1) to 36.2 % (Q3) (Fig. 8).

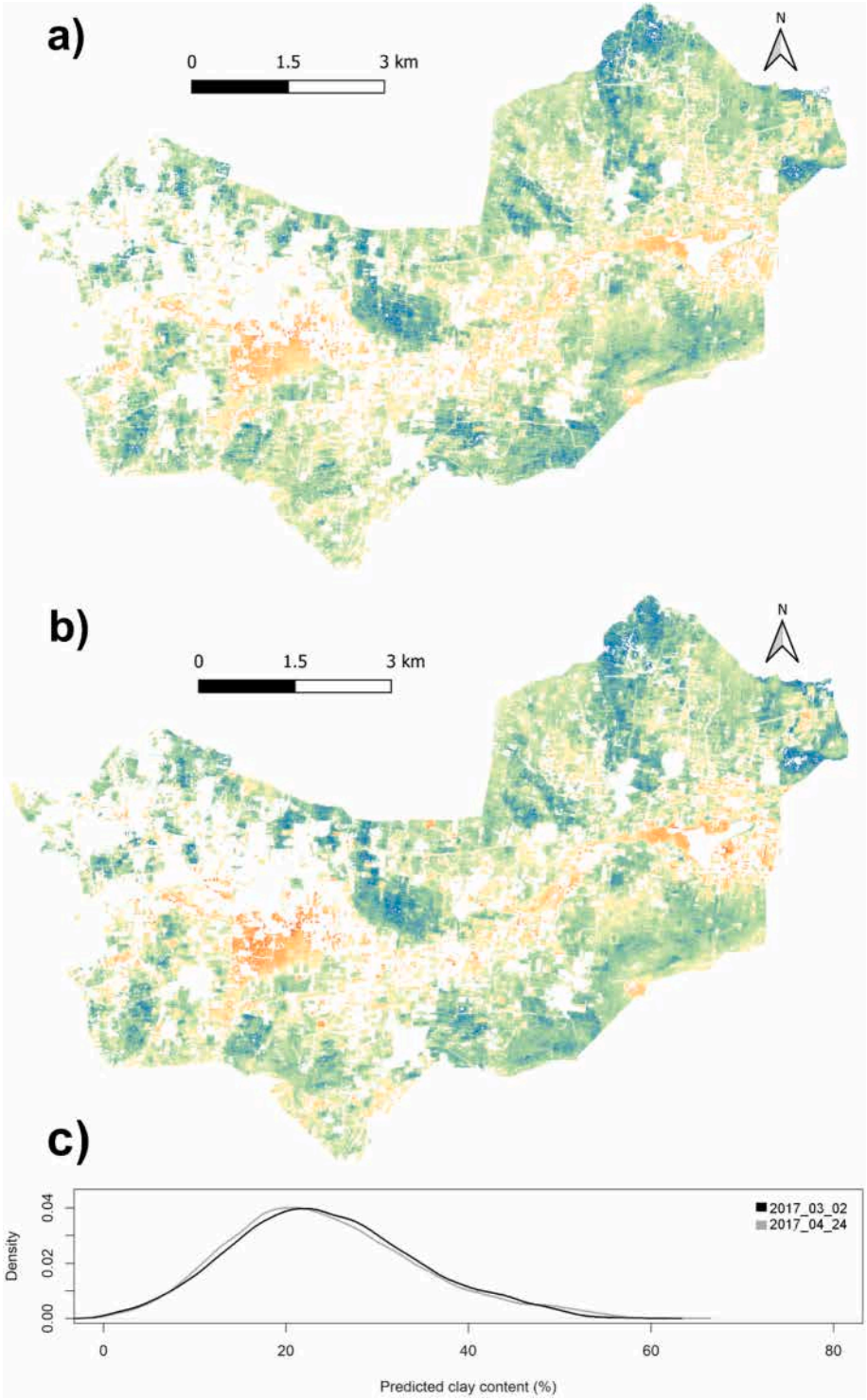

Fig. 4. Predicted clay content map a) on the 2017–02-03, b) on the 2017–04-24 and c) density graph of predicted clay content from both images.

Thus, more fields with sediment application were detected with the clay content change approach compared to the soil colour change approach. In addition, the clay-based approach allowed detecting applications over a wider range of initial clay content values while the colour-based approach was mostly effective when the initial clay content was low.

Among the 208 fields detected with a significant decrease of predicted clay content, only 166 could be studied with the soil colour change map while the other 42 did not match the criteria of 30 % of coverage in bare soil with the soil colour change map. Among these 166 fields, 22 were also detected with a soil colour change from "Black" to "Red", while for the remaining 144 fields, no colour change was detected. The decrease in the clay content was small, and not significantly different between the two groups (Wilcoxon Signed-Rank tests, p-value = 0.2807) (Fig. 9a). The mean initial clay content was not significantly different (Wilcoxon Signed-Rank tests, p-value = 0.8062) between the two groups. The range was much larger when the application was detected only with clay content changes, suggesting that, as for clay content increases, the method based on soil colour can detect changes only on a narrow range of initial clay content (Fig. 9b).

Table 2
Number of fields among control fields (19 without sediment application and 43 with sediment application) meeting (the one with 19 control fields without sediment application and the one with 43 control fields with sediment application) meeting criteria based on the clay-based approach.

	19 control fields without sediment application	43 control fields with sediment application
Number of fields with significant clay content decrease between t_1 and t_2	0	0
Number of fields with clay content differences inside the confidence interval [CI_{inf}; CI_{sup}]	18	5
Number of fields with significant clay content increase between t_1 and t_2	1	38

4. Discussion

4.1. Clay content mapping accuracies

The regression models for clay content estimations that we obtained from both Sentinel-2 images provided good performances regarding the figures of merit (Table 1). Moreover, these performances are in accordance with the ones obtained in literature with Sentinel-2 data. Our R^2 values fall within the same range as those of Gomez et al. (2022) (R^2 between 0.7 and 0.8) and Gasmi et al. (2022) (R^2 of 0.71) and are slightly higher than those reported by Bellinaso et al. (2021), Vaudour et al. (2019a) and the average values of Castaldi et al. (2023). RPIQ of our models are slightly lower than the one of Gasmi et al. (2022) (RPIQ of 3.01), while they are higher than in Bellinaso et al. (2021) (RPIQ of 1.86) and Castaldi et al. (2023) (RPIQ of 2.50). Finally, our RPD values are close to the one of Gasmi et al. (2022) and higher than the values in Vaudour et al. (2019b) (RPD from 1.0 to 1.5).

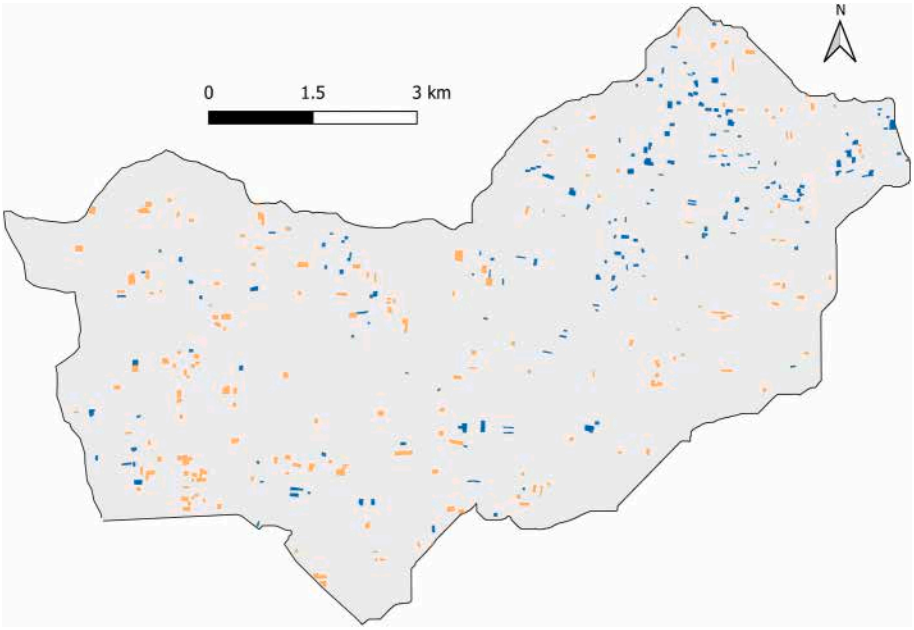

Fig. 5. 208 (in blue) and 242 (in orange) fields presenting a significant decrease and increase of predicted clay content following the criteria respectively.

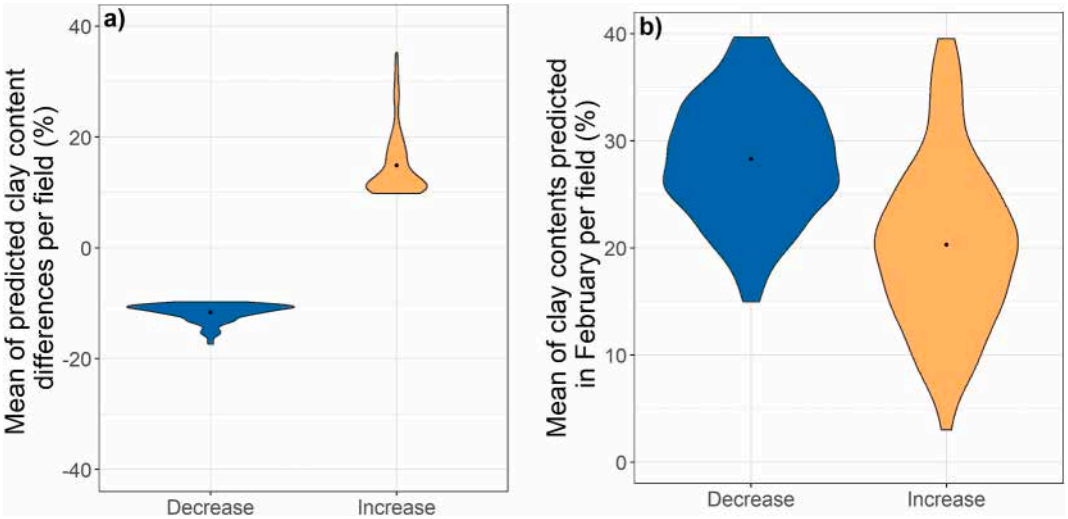

Fig. 6. Violin plots for the 208 (in blue) and 242 (in orange) fields presenting a significant decrease and increase of predicted clay content following the criteria, respectively. a) mean of predicted clay content differences per field, b) mean of initial clay content predicted in February per field.

Table 3
Number of fields among the control fields from both validation datasets (the one with 19 control fields without sediment application and the one with 43 control fields with sediment application) meeting criteria based on the soil colour changes approach.

Colour change	19 control fields without sediment application	42 control fields with sediment application existing on the soil colour change map
Number of fields with significant soil colour changes from Black to Red between t_1 and t_2	1	0
Number of fields with no soil colour changes	18	25
Number of fields with significant soil colour changes from Red to Black between t_1 and t_2	0	17

Both models are calibrated on bare soils that have not received any sediment, and similarly, they are validated on bare soils that have not received sediment. Checking the validity of the models specifically on soils with sediment would have improved our confidence in the precise estimation of clay content on these soils with sediment and would also allow us to quantify the clay content changes. However, this is beyond the scope of this paper, as we aim at using these significant variations of clay content as a proxy to detect the practice and not to precisely quantify the clay variations. A future work might be to improve the estimation of clay content on soils that have received sediment to finally quantify the clay content changes over detected fields impacted by this practice.

These models are calibrated from couples of soil properties and remote sensing image with temporal mismatch, as soil samples were collected in 2019 and S2 images were acquired in 2017. This approach remains correct as models are trained on soils that have not received any sediment and clay is a perennial property. It also aligns with existing literature (e.g., Castaldi, 2021; Castaldi et al., 2023; Vaudour et al., 2021; Žížala et al., 2019).

Finally, our study follows a large literature using MLR and multi-spectral data (e.g., Gomez et al., 2022; Mirzaee et al., 2016; Wang et al., 2022b). However, for more in-depth methodological studies, such as optimizing predictions at each date, a non-parametric approach, as suggested by Swain et al. (2021) and Biney et al. (2022), could represent a valuable step forward.

4.2. Model uncertainties due to multi-dates analysis

As highlighted previously by Vaudour et al. (2019b), models performances may vary from a Sentinel-2 image to another acquired on the same area, due to soil surface condition, amongst which soil roughness exhibited the most significant influence in their study. Their SOC predictions were more accurate with Sentinel-2 images acquired during periods with low surface roughness, along with those with no crop residues and no preceding rainfall events. Gomez et al. (2022) also highlighted that the prediction accuracy is more influenced by soil surface conditions than by atmospheric conditions, since atmospheric correction models yield comparable performances. These differences in model performances from a Sentinel-2 image to another are generally not enough to affect the pattern of the spatial distribution of soil properties, but they can introduce slight variations of predicted soil properties in time.

In our case, 95.9 % of the total fields and 95 % of our 19 control fields without sediment application present a clay content difference inside the confidence interval proposed by Styc (2020), which confirms that variations due to environmental factors (moisture, roughness or atmospheric conditions) fall within the confidence interval, and as a consequence, variations greater than the confidence interval should be attributed to other causes, such as sediment applications.

4.3. Significant difference in clay content as an indicator of sediment application

We found that the detection of sediment application with the clay content approach was more consistent than a detection based on a soil colour change. This difference in robustness can first be explained by the fact that the colour-based approach is not able to detect sediment application on soil identified in February as “Black”. Secondly, the qualification for the soil colour calibration database based on the Munsell colour system includes a subjective dimension (Post et al., 1993) and possible errors, in particular for samples that are not clearly red or black soils but rather brown soil (Gomez et al., 2021). Several sediment applications were detected with the colour change approach but not with the clay content approach because of the strong threshold effect in the colour method, where a pixel colour change can be linked to a small spectral change, particularly if the initial clay content ranges between 25 and 30 %.

Comparing clay contents between two dates allows quantifying the impact of the practice on soil texture when the change is large enough.

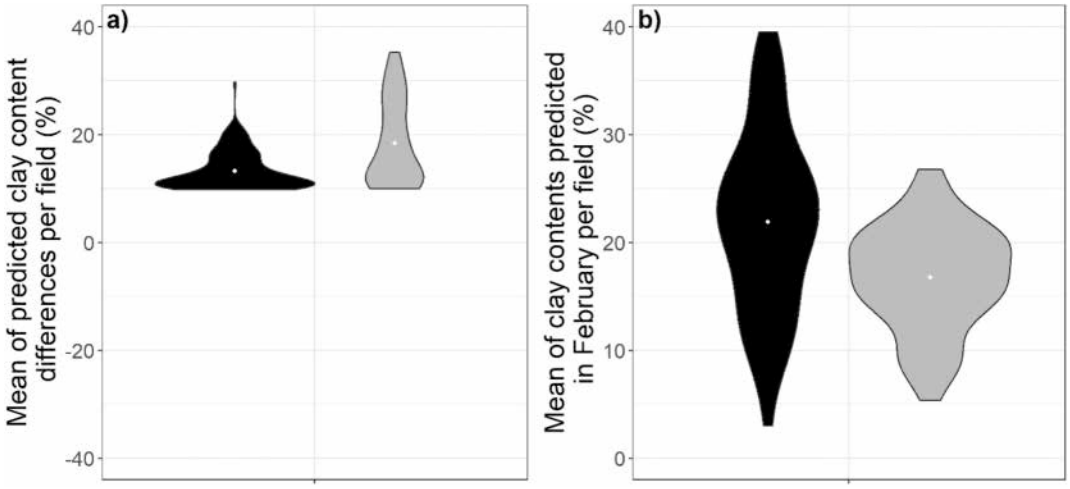

Fig. 7. Violin plots for the 69 fields (in grey) presenting both a significant increase of clay content and a change Red to Black colour, and the 152 (in black) presenting a significant increase of clay content and no soil colour change. a) mean of predicted clay content differences per field, b) mean of clay content predicted in February per field (all in %).

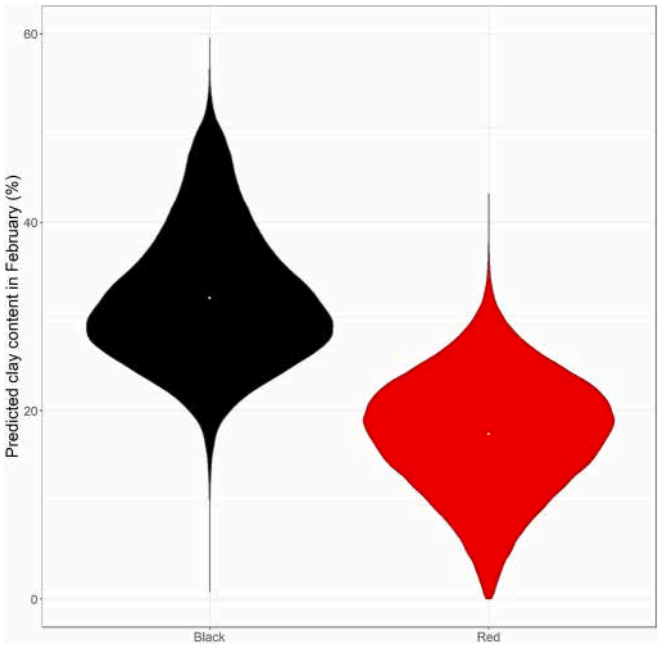

Fig. 8. Distribution of clay content predicted in February, for pixels associated to Red soil colour in February from classification approach (in red) and associated to Black soil colour in February from classification approach (in black).

Most of the control fields with sediment application could be detected with our method. The absence of a detection for five control fields is caused by the lack of a significant difference in clay content which can be due to the following reasons: an initial high clay content of the soil, a low clay content of the sediment and/or a low dose of sediments applied. First, Gomez et al. (2025) observed that the texture of the sediments collected in reservoirs in the Berambadi watershed varies from Sandy Clay Loam to Clay in the USDA soil textural triangle, and also observed a high variability of sediment application dose across individual farmers. As observed by Barbiero et al. (2010), soil textures in the Berambadi watershed vary from coarse (Sandy Loam over Ferralsols and Chromic Luvisols) to fine (Clay over Vertisols and Vertic intergrades). Based on our soil sample dataset, the clay content in the Berambadi watershed exhibits a wide, unimodal distribution centered around 22.5 %, corresponding to a Sandy Clay Loam texture. Therefore, the texture of the sediment might not always differ sufficiently from that of the soil to significantly affect the soil clay content, and even if the difference is large, the quantity applied might not always be sufficient. We can be confident that the method accurately classified fields with sediment application. However, this method might underestimate the extent of the practice, as it detects the sediment applications only if they have a sufficient impact on soil texture. Moreover, the number of fields identified as having received sediment in 2017 is also likely underestimated by our approach, as it focuses only on pixels covered by bare soil. Indeed, vegetated soil pixels are masked in soil properties mapping approach as dry and green vegetation are known to interfere with spectral measurements and compromise the accuracy of soil property predictions (Bartholomeus et al., 2011, Ouerghemmi et al., 2011, 2016). Finally, the time window between the two Sentinel-2 images limits sediment detection, leading to an underestimation of the practice. Sediment applications before 2017-03-02 remain undetectable, as any potential clay content increase would have occurred earlier than the first Sentinel-2 image. A multi-temporal approach with a wider time window could capture more applications within a dry season. Nevertheless, in 2017, the Sentinel-2 image from the 03-02 was the earliest usable one, as no earlier image matched the dry season (starting in January) with a long enough rain-free and cloud-free period to ensure reliable predictions.

The detection of 22 fields with both a significant decrease in clay content and a change from 'Black' to 'Red' suggests that some agricultural practices can reduce clay content, such as deep ploughing or an application of sandy sediment. Sediments from water reservoirs over Berambadi watershed exhibit contrasting physico-chemical properties from one reservoir to another (Gomez et al., 2025). Sediments collected from low clayey reservoirs (e.g., Gopalapura reservoir) could induce an increase in clay content only if applied to sandy soils, but may induce the opposite effect if applied to soils with greater clay content. Moreover, farmers in this region practice cropland leveling via sandy sediment application which can strongly affect the physical and chemical properties of the plough layer (Aschonitis et al., 2012, Fuentes-Guevara et al., 2022 and Oztekin, 2013). Another possible explanation is that sediment applications occurred shortly prior to the first Sentinel-2 acquisition, resulting in high clay content predictions due to sediment piles on the 2017-02-03 image, followed by a decrease in April as the sediments are mixed with the soil.

4.4. *Toward an estimation of the spatio-temporal evolution of the practice*

Assuming that the year 2017 is representative of the extent of the

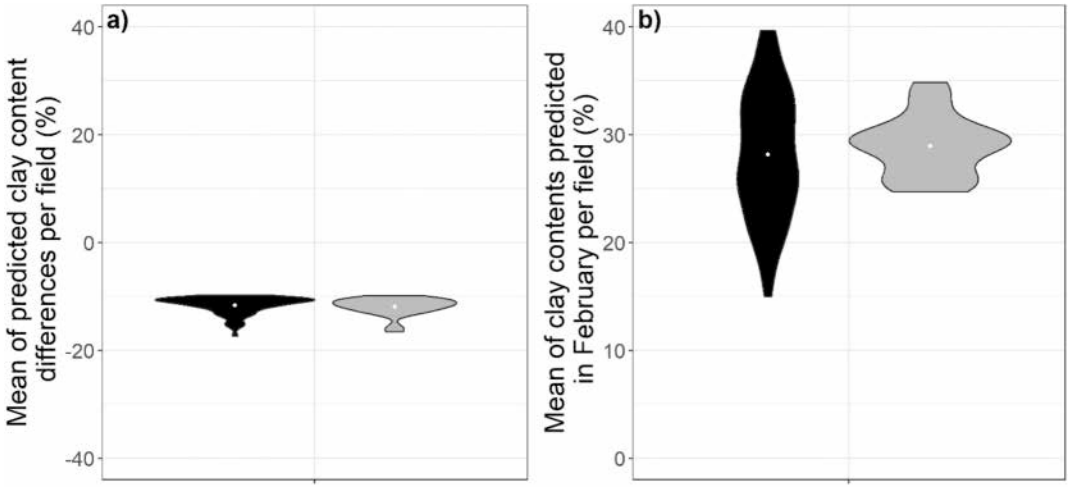

Fig. 9. Violin plots for the 22 fields (in grey) presenting a significant decrease of clay content and a change of soil colour from Black to Red, and the 144 (in black) presenting a significant decrease of clay content and no soil colour change. a) mean of predicted clay content differences per field, b) mean of clay content predicted in February per field (all in %).

practice, this suggests that around 2000 fields could have been amended with sediment from 2017 to 2024, accounting for approximately 12 % of the crop fields in the watershed. As sediment application occurs almost exclusively over irrigated fields (Gomez et al., 2025) and considering that less than 60 % of the farmers have access to irrigation (Robert et al., 2017), we can assume that around 20 % of the irrigable crop fields in the watershed have received sediments in the past 8 years, which is far from anecdotal. Beyond this first estimation based on one year (2017) and in order to evaluate the spatio-temporal evolution of the practice, it would be necessary to apply the method to different years, in addition to the first estimation based on one year (2017).

In this way, the characteristics of hydrological years, which may provide information on access to sediments, could help to map the practice. Indeed, the capacity of farmers to apply sediments depends, among others, on hydrological factors: excavators and tractors can access sediments only if the reservoirs are fully or at least partially dry during the summer season, which is not always the case.

One difficulty for applying the method to different years is that our method requires an accurate field boundary delineation. For this paper, we detected sediment applications at watershed scale using a field boundary delineation based on a layer which may have some errors as 1) it contains a significant number of polygons (18,146) of which 16,612 belong to the category "agricultural land" and are used in this study, and 2) it was produced manually. Nevertheless, a visual check allowed us to estimate the high quality of this field boundary delineation and the use of a buffer was considered as a last step of quality assurance. Unfortunately, field boundary delineations were only available for the year 2017, thereby limiting the mapping of sediment application to that period. This constitutes a limitation for reproducing our methodology as it stands over a multi-year time series. Remedying this problem by producing a field boundary delineation for every year would be extremely labour-intensive. Moreover, while application of deep learning on optical remote sensing data may lead to successful delineation of field boundaries in industrial agricultural systems (e.g, Yan and Roy, 2014), the same approach dedicated to smallholder systems may lead to poor quality delineation due to i) small fields that require high resolution satellite imagery (e.g., Sharma et al., 2018) and ii) lack of ground labels for model training and validation (e.g., Wang et al., 2022a). Thus, in order to ensure a better reproducibility of the method, the next step might be to develop a method for detecting the practice without using an agricultural field delineation, for example by using pixel clusters. First, it would improve our understanding of the practice in the Berambadi watershed (variations related to hydrologic conditions, possible recent expansion of the practice). Secondly, developing a more reproducible method would also allow applying the method to larger areas, in India or elsewhere, for assessing the spread of the practice in space and time and better understand its impact on soils and its overall sustainability.

4.5. Sentinel-2 as a major tool to study short-and long-term changes in soil properties at varying spatial scales?

In this study, we demonstrated the ability of Sentinel-2 data to detect significant short-term variations in clay content at the field scale within a watershed, resulting from sediment spreading on agricultural land. This opens new perspectives for the monitoring of both short-and long-term changes in soil properties at varying spatial scales, based on multi-temporal series of multispectral images such as Sentinel-2. Its good spatial resolution (10–20 m) might enable the detection of soil properties variations on relatively small entities such as smallholders' agricultural fields. Moreover, Sentinel-2 presents a 5-day revisit time which increases the probability of acquiring cloud-free images within short time windows. Based on promising works showing the potential of Sentinel-2 data for soil organic carbon (SOC) mapping (e.g., Vaudour et al., 2021), the detection of short-term variations in organic carbon due to agricultural practices such as compost or biochar inputs (e.g., Bellè et al., 2022), could be explored by Sentinel-2 data. The feasibility would depend, as in our work, on the performances of the SOC prediction models and also on the amplitude of the SOC changes induced by these practices, which must be higher than the residual-based confidence interval. Long-term variations of soil properties at field scale could also be studied, such as long-term changes in soil organic carbon stocks due to deforestation (Grinand et al., 2017). These scenarios concern variations on specific limited areas (fields or forest plots). This implies that a single training dataset with samples collected over pixels of unaffected areas of the study zone remains valid across multiple images for predictive modeling. Studies of extensive and short-term disturbances, such as large-scale erosion following exceptional flooding events, could be explored by estimating changes of soil texture due to widespread silt deposition (Li et al., 2024). In this latter scenario, separate training datasets would be required for each monitoring date to account for the altered soil conditions. Finally, across all scenarios, variations of soil properties studied have to be great enough to exceed model uncertainty thresholds, to ensure robust and meaningful monitoring.

5. Conclusion

This study evaluated the potential of Sentinel-2 time series to detect significant increases in soil clay content resulting from anthropogenic interventions such as sediment application. We successfully mapped the spatial extent of the agricultural practice at field scale for a given cropping season. These results underscore the value of Sentinel-2′s high temporal resolution and spectral capabilities for capturing short-term soil property changes. It also demonstrates the superiority of our method based on the clay content increase detection, compared to the previous approach based on soil colour change.

However, the clay prediction models were calibrated for specific dates and locations, highlighting the need for site- and time-specific ground data to improve transferability. Future research using the full Sentinel-2 archive (2017–present) could allow exploration of the spatio-temporal dynamics of sediment reuse over multiple years, which could be related to the climatic or socio-economic context. More broadly, this work opens ways for monitoring both short- and long-term soil property changes (beyond clay content) at varying spatial scales using multi-temporal multispectral data.

Declaration of Generative AI and AI-assisted technologies in the writing process

During the preparation of this work the authors used DeepL and Grammarly in order to improve the language of the manuscript. After using this tool, the authors reviewed and edited the content as needed and take full responsibility for the content of the published article.

CRediT authorship contribution statement

J. Gaab: Writing – review & editing, Writing – original draft, Visualization, Validation, Software, Methodology, Investigation, Formal analysis, Data curation. **L. Ruiz:** Writing – review & editing, Visualization, Validation, Supervision, Methodology, Formal analysis, Conceptualization. **M. Sekhar:** Writing – review & editing, Resources. **S. Dharumarajan:** Writing – review & editing, Resources. **J.Masika Tutondele:** Writing – review & editing. **M.Ebengo Okoto:** Writing – review & editing. **C. Gomez:** Writing – review & editing, Visualization, Validation, Supervision, Resources, Methodology, Funding acquisition, Formal analysis, Conceptualization.

Declaration of competing interest

The authors declare that they have no known competing financial interests or personal relationships that could have appeared to influence

the work reported in this paper.

Acknowledgements

This research was supported by the project “4S” from the Roullier Endowment Fund and the PNTS 2023-08 “TankSed”. The authors are indebted to NBSS&LUP for soil samples collection. The Kabini Critical Zone Observatory (AMBHAS, BVET, Sekhar et al., 2016; Tomer et al., 2015, www.ambhas.com; https://mtropics.obsmip.fr/), which is part of the OZCAR network (Gaillardet et al., 2018, http://www.ozcar-ri.org/ozcar/), are also acknowledged. We acknowledge the Institut Agro Montpellier (France) for the PhD fellowship financed by the French Ministry of Agriculture.

Appendix A. Supplementary material

Supplementary data to this article can be found online at https://doi.org/10.1016/j.geoderma.2025.117630.

Data availability

Data will be made available on request.

References

AMBHAS Team, 2015. A Manual for Agro-Hydrological Monitoring in Pilot Experimental Watersheds. Indian Institute of Sciences and AMBHAS August 2015. 65 pages. https://watershed.karnataka.gov.in/storage/pdf-files/Sujala%20Docs/Hydrology%20Manual.pdf.

Aschonitis, V.G., Kostopoulou, S.K., Antonopoulos, V.Z., 2012. Methodology to assess the effects of rice cultivation under flooded conditions on van Genuchten's model parameters and pore size distribution. Transp. Porous Media 91, 861–876. https://doi.org/10.1007/s11242-011-9876-9.

Baccar, M., Raynal, H., Sekhar, M., Bergez J-E., Willaume, M., Casel, P., Giriraj, P., Murthy, S., Ruiz, L., 2023, Dynamics of crop category choices reveal strategies and tactics used by smallholder farmers in India to cope with unreliable water availability, Agricult. Syst. 211, 103744,ISSN 0308-521X, https://doi.org/10.1016/j.agsy.2023.103744.

Barbiero, L., Mohan Kumar, M.S., Violette, A., Oliva, P., Braun, J.J., Kumar, C., Furian, S., Babic, M., Riotte, J., Valles, V., 2010. Ferrolysis induced soil transformation by natural drainage in Vertisols of sub-humid South India. Geoderma 156 (3–4), 173–188. https://doi.org/10.1016/j.geoderma.2010.02.014.

Bartholomeus, H., Kooistra, L., Stevens, A., Van Leeuwen, M., VanWesemael, B., Ben-Dor, E., Tychon, B., 2011. Soil organic carbon mapping of partially vegetated agricultural fields with imaging spectroscopy. Int. J. Appl. Earth Obs. Geoinf. 13, 81–88. https://doi.org/10.1016/j.jag.2010.06.009.

Bégué, A., Vintrou, E., Saad, A., Petit, C., 2018. Remote sensing and cropping practices monitoring: the case of crop rotation and tillage monitoring. Eur. J. Agron. 98, 73–80. https://doi.org/10.3390/rs10010099.

Bellè, S.-L., Riotte, J., Backhaus, N., Sekhar, M., Jouquet, P., Abiven, S., 2022. Tailor-made biochar systems: interdisciplinary evaluations of ecosystem services and farmer livelihoods in tropical agro-ecosystems. PLoS One 17 (1), e0263302. https://doi.org/10.1371/journal.pone.0263302.

Bellinaso, H., Silvero, N.E., Ruiz, L.F.C., Accorsi Amorim, M.T., Rosin, N.A., de Sousa Mendes, W., de Sousa, G.P.B., Sepulveda, L.M.A., de Queiroz, L.G., Nanni, M.R., Demattê, J.A., 2021. Clay content prediction using spectra data collected from the ground to space platforms in a smallholder tropical area. Geoderma 399, 115116. https://doi.org/10.1016/j.geoderma.2021.115116.

Bellon-Maurel, V., Fernandez-Ahumada, E., Palagos, B., Roger, J.-M., McBratney, A., 2010. Critical review of chemometric indicators commonly used for assessing the quality of the prediction of soil attributes by NIR spectroscopy. Trends Anal. Chem. 29, 1073–1081. https://doi.org/10.1016/j.trac.2010.05.006.

Biney, J.K.M., Vasat, R., Bell, S.M., Kebonye, N.M., Klement, A., John, K., Borůvka, L., 2022. Prediction of topsoil organic carbon content with Sentinel-2 imagery and spectroscopic measurements under different conditions using an ensemble model approach with multiple pre-treatment combinations. Soil Tillage Res. 220, 105379. https://doi.org/10.1016/j.still.2022.105379.

Canet, R., Chaves, C., Pomares, F., Albiach, R., 2003. Agricultural use of Sediments from the Albufera Lake (Eastern Spain). Agric. Ecosyst. Environ. 95 (1), 29–36. https://doi.org/10.1016/S0167-8809(02)00171-8.

Castaldi, F., 2021. Sentinel-2 and Landsat-8 multi-temporal series to estimate topsoil properties on croplands. Remote Sens. (Basel) 13, 3345. https://doi.org/10.3390/rs13173345.

Castaldi, F., Koparan, M.H., Wetterlind, J., Žydelis, R., Vinci, I., Savaş, A.Ö., Kıvrak, C., Tunçay, T., Volungevičius, J., Obber, S., Ragazzi, F., Malo, D., Vaudour, E., 2023. Assessing the capability of Sentinel-2 time-series to estimate soil organic carbon and clay content at local scale in croplands. ISPRS J. Photogramm. Remote Sens. 199, 40–60. https://doi.org/10.1016/j.isprsjprs.2023.03.016.

Chabrillat, S., Goetz, A.F.H., Krosley, L., Olsen, H.W., 2002. Use of hyperspectral images in the identification and mapping of expansive clay soils and the role of spatial resolution. Remote Sens. Environ. 82 (2), 431–445. https://doi.org/10.1016/S0034-4257(02)00060-3.

Chang, C.-W., Laird, D.A., Mausbach, M.J., Hurburgh, C.R., 2001. Near-infrared reflectance Spectroscopy–principal components regression analyses of soil properties. Soil Sci. Soc. Am. J. 65 (2), 480–490. https://doi.org/10.2136/sssaj2001.652480x.

Daughtry, C.S.T., Hunt, E.R., McMurtrey, J.E., 2004. Assessing crop residue cover using shortwave infrared reflectance. Remote Sens. Environ. 90 (1), 126–134. https://doi.org/10.1016/j.rse.2003.10.023.

Deshmukh, D.P., Deshmukh, P.W., Bhoyar, S.M., Gawai, S.P., 2019. Characterization of physical attributes of tank silt of natural reservoirs in western Melghat region of Dharni. Int. J. Chem. Stud. 7 (3), 2782–2785.

Deshpande, M.V., Pillai, D., Krishna, V.V., Jain, M., 2024. Detecting and quantifying zero tillage technology adoption in Indian smallholder systems using Sentinel-2 multispectral imagery. Int. J. Appl. Earth Obs. Geoinf. 128, 103779. https://doi.org/10.1016/j.jag.2024.103779.

Deventer, V., Ward, A., Gowda, P., Lyon, J., 1997. Using thematic mapper data to identify contrasting soil plains and tillage practices. Am. Soc. Photogr. Remote Sens. 63, 87–93.

DHAN Foundation (2012). Policy brief 12. Tank sediment Application 638 for Agricultural Production 639 Enhancement- Scope, Issues and Challenges. Proposed by The DHAN Foundation.

Dodin, M., Smith, H.D., Levavasseur, F., Hadjar, D., Houot, S., Vaudour, E., 2021. Potential of sentinel-2 satellite images for monitoring green waste compost and manure amendments in temperate cropland. Remote Sensing (basel) 13, 1616. https://doi.org/10.3390/rs13091616.

Dray, S., Dufour, A.B., 2007. The ade4 package: implementing the duality diagram for ecologists. J. Stat. Softw. 22, 1–20. https://doi.org/10.18637/jss.v022.i04.

Dvorakova, K., Heiden, U., Pepers, K., Staats, G., van Os, G., van Wesemael, B., 2023. Improving soil organic carbon predictions from a sentinel–2 soil composite by assessing surface conditions and uncertainties. Geoderma 429, 116128. https://doi.org/10.1016/j.geoderma.2022.116128.

Fischer, C., Aubron, C., Trouvé, A., Sekhar, M., Ruiz, L., 2022. Groundwater irrigation reduces overall poverty but increases socioeconomic vulnerability in a semiarid region of southern India. Scientific reports 12, 8850 (2022). https://doi.org/10.1038/s41598-022-12814-0.

Frampton, W.J., Dash, J., Watmough, G., Milton, E.J., 2013. Evaluating the capabilities of Sentinel-2 for quantitative estimation of biophysical variables in vegetation. ISPRS J. Photogramm. Remote Sens. 82, 83–92. https://doi.org/10.1016/j.isprsjprs.2013.04.007.

Fuentes-Guevara, M., Armindo, R., Timm, L., Faria, L., 2022. Examining the land leveling impacts on the physical quality of lowland soils in Southern Brazil. Soil Tillage Res. 215, 105217. https://doi.org/10.1016/j.still.2021.105217.

Gaillardet, J., Braud, I., Hankard, F., Anquetin, S., Bour, O., Dorfliger, N., de Dreuzy, J.R., Galle, S., Galy, C., Gogo, S., Gourcy, L., Habets, F., Laggoun, F., Longuevergne, L., Le Borgne, T., Naaim-Bouvet, F., Nord, G., Simonneaux, V., Six, D., Tallec, T., Valentin, C., Abril, G., Allemand, P., Arènes, A., Arfib, B., Arnaud, L., Arnaud, N., Arnaud, P., Audry, S., Comte, V.B., Batiot, C., Battais, A., Bellot, H., Bernard, E., Bertrand, C., Bessière, H., Binet, S., Bodin, J., Bodin, X., Boithias, L., Bouchez, J., Boudevillain, B., Moussa, I.B., Branger, F., Braun, J.J., Brunet, P., Caceres, B., Calmels, D., Cappelaere, B., Celle-Jeanton, H., Chabaux, F., Chalikakis, K., Champollion, C., Copard, Y., Cotel, C., Davy, P., Deline, P., Delrieu, G., Demarty, J., Dessert, C., Dumont, M., Emblanch, C., Ezzahar, J., Estèves, M., Favier, V., Faucheux, M., Filizola, N., Flammarion, P., Floury, P., Fovet, O., Fournier, M., Francez, A.J., Gandois, L., Gascuel, C., Gayer, E., Genthon, C., Gérard, M.F., Gilbert, D., Gouttevin, I., Grippa, M., Gruau, G., Jardani, A., Jeanneau, L., Join, J.L., Jourde, H., Karbou, F., Labat, D., Lagadeuc, Y., Lajeunesse, E., Lastennet, R., Lavado, W., Lawin, E., Lebel, T., Le Bouteiller, C., Legout, C., Lejeune, Y., Le Meur, E., Le Moigne, N., Lions, J., Lucas, A., Malet, J.P., Marais-Sicre, C., Maréchal, J.C., Marlin, C., Martin, P., Martins, J., Martinez, J.M., Massei, N., Mauclerc, A., Mazzilli, N., Molénat, J., Moreira-Turcq, P., Mougin, E., Morin, S., Ngoupayou, J.N., Panthou, G., Peugeot, C., Picard, G., Pierret, M.C., Porel, G., Probst, A., Probst, J.L., Rabatel, A., Raclot, D., Ravanel, L., Rejiba, F., René, P., Ribolzi, O., Riotte, J., Rivière, A., Robain, H., Ruiz, L., Sanchez-Perez, J.M., Santini, W., Sauvage, S., Schoeneich, P., Seidel, J.L., Sekhar, M., Sengtaheuanghoung, O., Silvera, N., Steinmann, M., Soruco, A., Tallec, G., Thibert, E., Lao, D.V., Vincent, C., Viville, D., Wagnon, P., Zitouna, R., 2018. OZCAR: the French network of critical zone observatories. Vadose Zone J. 17 (1), 180067. https://doi.org/10.2136/vzj2018.04.0067.

Gao, F., Anderson, M.C., Hively, W.D., 2020. Detecting cover crop end-of-season using VENμS and Sentinel-2 satellite imagery. Remote Sens. (Basel) 12 (21), 3524. https://doi.org/10.3390/rs12213524.

Gasmi, A., Gomez, C., Lagacherie, P., Zouari, H., Laamrani, A., Chehbouni, A., 2021. Mean spectral reflectance from bare soil pixels along a Landsat-TM time series to increase both the prediction accuracy of soil clay content and mapping coverage, Geoderma, 388, 114864, ISSN 0016-7061, https://doi.org/10.1016/j.geoderma.2020.114864.

Gasmi, A., Gomez, C., Chehbouni, A., Dhiba, D., el Fil, H., 2022. Satellite multi-sensor data fusion for soil clay mapping based on the spectral index and spectral bands approaches. Remote Sens. 14, 1103. https://doi.org/10.3390/rs14051103.

Google Earth Pro, 2025. Satellite image Berambadi. Imagery dates: 2017-02-23, 2017-02-24, 2017-02-27. Image © 2025 Maxar Technologies. Google. https://earth.google.com.

Gomez, C., Adeline, K., Bacha, S., Driessen, B., Gorretta, N., Lagacherie, P., Roger, J.M., Briottet, X., 2018. Sensitivity of clay content prediction to spectral configuration of VNIR/SWIR imaging data, from multispectral to hyperspectral scenarios. Remote Sens. Environ. 204, 18–30. https://doi.org/10.1016/j.rse.2017.10.047.

Gomez, C., Dharumarajan, S., Féret, J.-B., Lagacherie, P., Ruiz, L., Sekhar, M., 2019. Use of Sentinel-2 time-series images for classification and uncertainty analysis of inherent biophysical property: case of soil texture mapping. Remote Sens. (Basel) 11 (5), 565. https://doi.org/10.3390/rs11050565.

Gomez, C., Dharumarajan, S., Lagacherie, P., Riotte, J., Ferrant, S., Sekhar, M., Ruiz, L., 2021. Mapping of tank silt application using Sentinel-2 images over the Berambadi catchment (India). Geoderma Reg. 25, e00389. https://doi.org/10.1016/j.geodrs.2021.e00389.

Gomez, C., Vaudour, E., Féret, J.-B., de Boissieu, F., Dharumarajan, S., 2022. Topsoil clay content mapping in croplands from Sentinel-2 data: influence of atmospheric correction methods across a season time series. Geoderma 423, 115959. https://doi.org/10.1016/j.geoderma.2022.115959.

Gomez, C., Amelin, J., Coulouma, G., Gaab, J., Dharumarajan, S., Riotte, J., Sekhar, M., Ruiz, L., 2025. Reuse of bottom sediment from reservoirs to cropland is a promising agroecological practice that must be rationalized. Sci. Rep. 15, 7523. https://doi.org/10.1038/s41598-025-92206-2.

Grinand, C., Le Maire, G., Vieilledent, G., Razakamanarivo, H., Razafimbelo, T., Bernoux, M., 2017. Estimating temporal changes in soil carbon stocks at ecoregional scale in Madagascar using remote-sensing. Int. J. Appl. Earth Observat. Geoinformat. 54, February 2017, Pages 1-14. https://doi.org/10.1016/j.jag.2016.09.002.

Gunnell, Y., Krishnamurthy, A., 2003. Past and present status of runoff harvesting systems in dryland Peninsular India: a critical review. J. Human Environ. 32(4), 320–324. https://doi.org/10.1579/0044-7447-32.4.320.

Hagolle, O., Huc, M., Desjardins, C., Auer, S., Richter, R., 2017. MAJA Algorithm Theoretical Basis Document. CNES, CESBIO & DLR. Report ref MAJA-TN-WP2-030 Issue 1.0. https://www.theia-land.fr/sites/default/files/imce/produits/atbd_maja_071217.pdf.

Hemingway, C., Ruiz, L., Vigne, M., Aubron, C., 2025. The changing role of livestock in agrarian systems: A historical and multifunctional perspective from southern India. Agronomy for Sustainable Development 45:7, 16 p. https://doi.org/10.1007/s13593-024-00999-9.

Heuvelink, G.B.M., 2014. Uncertainty quantification of GlobalSoilMap products. In: Arrouays, D., McKenzie, N.J., Hempel, J., Richer-de-Forges, A.C., McBratney, A.B. (Eds.), GlobalSoilMap. Basis of the global soil information system. Taylor & Francis, CRC Press, London, pp. 335–340. https://doi.org/10.1201/b16500-62.

Kariuki, P.C., Woldai, T., Van Der Meer, F., 2004. Effectiveness of spectroscopy in identification of swelling indicator clay minerals. Int. J. Remote Sens. 25 (2), 455–469. https://doi.org/10.1080/0143116031000084314.

Li, J., Wang, G., Song, C., Sun, S., Ma, J., Wang, Y., Guo, L., Li, D., 2024. Recent intensified erosion and massive sediment deposition in Tibetan Plateau rivers. Nat. Commun. 15, 722. https://doi.org/10.1038/s41467-024-44982-0.

Lonjou, V., Desjardins, C., Hagolle, O., Petrucci, B., Tremas, T., Dejus, M., Makarau, A., Auer, S., 2016. "MACCS-ATCOR joint algorithm (MAJA)", Proc. SPIE 10001, Remote Sensing of Clouds and the Atmosphere XXI, 1000107 (19 October 2016). https://doi.org/10.1117/12.2240935.

Mark, H.L., Tunnell, D., 1985. Qualitative near-infrared reflectance analysis using Mahalanobis distances. Anal. Chem. 57, 1449–1456.

Mevik, B.-H., Wehrens, R., 2007. The pls Package: principal component and partial least squares regression in R. J. Stat. Softw. 18, 1–24. https://doi.org/10.18637/jss.v018.i02.

Mirzaee, S., Ghorbani-Dashtaki, S., Mohammadi, J., Asadi, H., Asadzadeh, F., 2016. Spatial variability of soil organic matter using remote sensing data. Catena 145, 118–127. https://doi.org/10.1016/j.catena.2016.05.023.

Montgomery, D. C., Peck, E. A., & Vining, G. G. (2012). Introduction to Linear Regression Analysis (5th ed.). Wiley.

Ouerghemmi, W., Gomez, C., Naceur, S., Lagacherie, P., 2011. Applying blind source separation on hyperspectral data for clay content estimation over partially vegetated surfaces. Geoderma 163, 227–237. https://doi.org/10.1016/j.geoderma.2011.04.019.

Ouerghemmi, W., Gomez, C., Naceur, S., Lagacherie, P., 2016. Semi-blind source separation for the estimation of the clay content over semi-vegetated areas using VNIR/SWIR hyperspectral airborne data. Remote Sens. Environ. 181, 251–263. https://doi.org/10.1016/j.rse.2016.04.013.

Oztekin, T., 2013. Short-term effects of land leveling on irrigation-related some soil properties in a clay loam soil. Sci. World J. 2013, 1–16. https://doi.org/10.1155/2013/187490.

Pérez, C.C., Olthoff, A.E., Hernandez-Trejo, H., Rullan-Silva, C.D., 2022. Evaluating the best spectral indices for burned areas in the tropical Pantanos de Centla Biosphere Reserve, Southeastern Mexico. Remote Sens. Appl.-Soc. Environ. 25, 100664–100677. https://doi.org/10.1016/j.rsase.2021.100664.

Piper, C.S., 1966. Soil and Plant Analysis. Hans Publisher, Bombay.

Post, D. F., Bryant, R. B., Batchily, A. K., Huete, A. R., Levine, S. J., Mays, M. D., Escadafal, R. (1993). Correlations Between Field and Laboratory Measurements of Soil Color. In J. M. Bigham & E. J. Ciolkosz (Éds.), SSSA Special Publications (p. 35–49). Soil Science Society of America. https://doi.org/10.2136/sssaspecpub31.c3.

Reddy, V.R., Reddy, M.S., Palanisami, K., 2018. Tank rehabilitation in India: review of experiences and strategies. Agric Water Manage 209, 32–43. https://doi.org/10.1016/j.agwat.2018.07.013.

Robert, M., Thomas, A., Sekhar, M., Badiger, S., Ruiz, L., Willaume, M., Leenhardt, D., Bergez, J.E., 2017. Farm typology in the Berambadi Watershed (India): Farming systems are determined by farm size and access to groundwater. Water 2017 (9), 51. https://doi.org/10.3390/w9010051.

Rouse, J.W., Haas, R.H., Schell, J.A., Deering, W.D. Monitoring vegetation systems in the Great Plains with ERTS. Third Earth Resources Technology Satellite-1 Symposium 1973, NASA SP-351, 309–317.

R Development Core Team, 2012. R: A Language and Environment for Statistical Computing. R foundation for Statistical Computing, Vienna. http://www.R-project.org/.

Schapper, H.P., 1957. Uses and limitations of farm surveys. Aust. J. Agric. Econ. 1 (1), 49–60. https://doi.org/10.1111/j.1467-8489.1957.tb00006.x.

Sekhar, M., Riotte, J., Ruiz, L., Jouquet, P., Braun, J.J., 2016. Influences of climate and agriculture on water and biogeochemical cycles: kabini critical zone observatory. Proc. Indian Natl. Sci. Acad. 82 (3), 833–846. https://doi.org/10.16943/ptinsa/2016/48488.

Sharma, A.K., Hubert-Moy, L., Buvaneshwari, S., Sekhar, M., Ruiz, L., Bandyopadhyay, S., Corgne, S., 2018. Irrigation history estimation using multitemporal landsat satellite images: application to an intensive groundwater irrigated agricultural Watershed in India. Remote Sens. (Basel) 10 (6), 893. https://doi.org/10.3390/rs10060893.

Silvero, N.E.Q., Dematte, J.A.M., Amorim, M.T.A., Santos, N.V., Rizzo, R., Safanelli, J.L., Poppiel, R.R., Mendes, W.S., Bonfatti, B.R., 2021. Soil variability and quantification based on Sentinel-2 and Landsat-8 bare soil images: a comparison. Remote Sens. Environ. 252, 112117. https://doi.org/10.1016/j.rse.2020.112117.

Srinivasarao, Ch., Rejani, R., Kumar, P., 2014. Climate resilient water management practices for improving water use efficiency and sustaining crop productivity. National Workshop, Climate Change & Water: Improving WUE. WALAMTARI, 13-14 Nov, 2014.

Stamatiadis, S., Liopa-Tsakalidi, A., Maniati, L. M., Karageorgou, P., Natioti, E., 1997. A Comparative Study of Soil Quality in Two Vineyards Differing in Soil Management Practices. In J. W. Doran & A. J. Jones (Éds.), SSSA Special Publications (p. 381–392). Soil Science Society of America.

Styc, Q. Cartographie numérique du Réservoir Utile en eau des sols à partir de données pédologiques anciennes : application à la plaine littorale Languedocienne. Science des sols. Institut national d'enseignement supérieur pour l'agriculture, l'alimentation et l'environnement, 2020. Français.

Swain S.R., Chakraborty P., Panigrahi N., Vasava H.B., Reddy N.N., Roy S., Majeed I., Das B.S., 2021. Estimation of soil texture using Sentinel-2 multispectral imaging data: An ensemble modeling approach, Soil and Tillage Research, 213, 105134, ISSN 0167-1987, https://doi.org/10.1016/j.still.2021.105134.

Tomer, S.K., Al Bitar, A., Sekhar, M., Zribi, M., Bandyopadhyay, S., Sreelash, K., Sharma, A.K., Corgne, S., Kerr, Y., 2015. Retrieval and multi-scale validation of soil moisture from multi-temporal SAR data in a semi-arid tropical region. Remote Sens. (Basel) 7, 8128–8153. https://doi.org/10.3390/rs70608128.

Tugel, A.J., Herrick, J.E., Brown, J.R., Mausbach, M.J., Puckett, W., Hipple, K., 2005. Soil change, soil survey, and natural resources decision making. Soil Sci. Soc. Am. J. 69, 738–747. https://doi.org/10.2136/sssaj2004.0163.

Vaudour, E., Gomez, C., Fouad, Y., Lagacherie, P., 2019a. Sentinel-2 image capacities to predict common topsoil properties of temperate and Mediterranean agroecosystems. Remote Sens. Environ. 223, 21–33. https://doi.org/10.1016/j.rse.2019.01.006.

Vaudour, E., Gomez, C., Loiseau, T., Baghdadi, N., Loubet, B., Arrouays, D., Ali, L., Lagacherie, P., 2019b. The impact of acquisition date on the prediction performance of topsoil organic carbon from Sentinel-2 for croplands. Remote Sens. (Basel) 11, 2143. https://doi.org/10.3390/rs11182143.

Vaudour, E., Gomez, C., Lagacherie, P., Loiseau, T., Baghdadi, N., Urbina-Salazar, D., Loubet, B., Arrouays, D., 2021. Temporal mosaicking approaches of Sentinel-2 images for extending topsoil organic carbon content mapping in croplands. Int. J. Appl. Earth Obs. Geoinf. 96, 102277. https://doi.org/10.1016/J.JAG.2020.102277.

Viscarra Rossel, R.A., Walvoort, D.J.J., McBratney, A.B., Janik, L.J., Skjemstad, J.O., 2006. Visible, near infrared, mid infrared or combined diffuse reflectance spectroscopy for simultaneous assessment of various soil properties. Geoderma 131 (1–2), 59–75. https://doi.org/10.1016/j.geoderma.2005.03.007.

Wang, A., Vikram R., Russakovsky, O. 2022. Towards Intersectionality in Machine Learning: Including More Identities, Handling Underrepresentation, and Performing Evaluation. In: Proceedings of the 2022 ACM Conference on Fairness, Accountability, and Transparency. 336–349. https://doi.org/10.1145/3531146.3533101.

Wang, B., Gray, J.M., Waters, C.M., Rajin Anwar, M., Orgill, S.E., Cowie, A.L., Feng, P., Li Liu, D., 2022b. Modelling and mapping soil organic carbon stocks under future climate change in south-eastern Australia. Geoderma 405, 115442. https://doi.org/10.1016/j.geoderma.2021.115442.

Wilding, L.P., Bouma, J., Goss, D.W., 1994. Impact of Spatial Variability on Interpretive Modeling. https://doi.org/10.2136/sssaspecpub39.c4.

Wold, S., Sjöström, M., Eriksson, L., 2001. PLS-regression: a basic tool of chemometrics. Chemom. Intel. Lab. Syst. 58 (2), 109–130. https://doi.org/10.1016/S0169-7439(01)00155-1.

Yan, L., Roy, D., 2014. Automated crop field extraction from multi-temporal Web Enabled Landsat Data. Remote Sens. Environ. 144, 42–64. https://doi.org/10.1016/j.rse.2014.01.006.

Žížala, D., Minařík, R., Zádorová, T., 2019. Soil organic carbon mapping using multispectral remote sensing data : prediction ability of data with different spatial and spectral resolutions. Remote Sens. (Basel) 11 (24), 2947. https://doi.org/10.3390/rs11242947.

Zhang, K., Li, X., Zheng, D., Zhang, L., Zhu, G., 2022. Estimation of Global Irrigation Water Use by the Integration of Multiple Satellite Observations. Water Resour. Res. 58 (3), e2021WR030031. https://doi.org/10.1029/2021WR030031.

Zhanguo Bai, Thomas Caspari, Maria Ruiperez Gonzalez, Niels H. Batjes, Paul Mäder, Else K. Bünemann, Ron de Goede, Lijbert Brussaard, Minggang Xu, Carla Sofia Santos Ferreira, Endla Reintam, Hongzhu Fan, Rok Mihelič, Matjaž Glavan, Zoltán Tóth,

Effects of agricultural management practices on soil quality: A review of long-term experiments for Europe and China, Agriculture, Ecosystems & Environment, Volume 265, 2018, Pages 1-7, ISSN 0167-8809, https://doi.org/10.1016/j.agee.2018.05.028.